Conformational Analysis of Major Metabolites of Macrolide Antibiotics Roxithromycin and Erythromycin A with Different Biological Properties by NMR Spectroscopy and Molecular Dynamics

Josyane Gharbi-Benarous, Patrick Ladam, Marcel Delaforge and Jean-Pierre Girault*
Université René Descartes, Laboratoire de Chimie et Biochimie Pharmacologiques et Toxicologiques, C.N.R.S. U.R.A. 400, 45 rue des Saints-Pères, F-75270 Paris cedex 06, France

The drugs roxithromycin **1** and erythromycin **2** differ in their ability to produce a hepatotoxic effect or drug interactions involving macrolide antibiotics. The major metabolite of **1**, RU39001 (**3**) does not induce hepatic cytochrome P-450 while the metabolite of **2**, erythralosamine (**4**) has greater interaction properties either *in vitro* or *in vivo* with the cytochrome P-450 system. A combination of NMR spectroscopy and molecular dynamics (MD) has shown that the conformations of **1** and **2**, in $CDCl_3$ solution, undergo an interesting conformational reorganization. The movement of the macrocycle induces five different orientations of the desosamine sugar. The use of MD simulation has facilitated the identification of conformations of their major metabolites in solution as predicted by NMR spectroscopy. There is a significant proportion of an active conformation for **4** and a conformation which can be related to the inhibition of cytochrome P-450 for **3**. These results also demonstrate the importance of the nature of hydrogen bonding for **1** and its metabolite **3** which may also explain some of the biological differences observed for **1** and **3** with respect to erythromycin **2** and its metabolite **4**. Similarly, the ionization of the amino group favouring one inactive conformation could allow changes in the motion and in the reactivity of the desosamine unit.

The therapeutic utility of macrolide antibiotics is well established[1] and erythromycin remains an important antimicrobial agent. Decomposition of erythromycin under acidic conditions has been thought to proceed *via* the 6,9:9,12-spiroketal.[2] Since the intramolecular cyclization of erythromycin destroys its antibiotic activity, much effort has been spent to reduce or completely block this degradative pathway. It should be noted that tautomeric forms of erythromycin A have been implicated in certain biological reactions of this molecule.[3] This type of tautomerism is not observed for 9-oximo derivatives[4] such as roxithromycin, a new macrolide antibiotic.[5,6] Roxithromycin has exhibited better pharmacokinetic characteristics such as increased stability to acid, greater oral bioavailability, higher serum concentrations, better tissue penetration and longer body half life than erythromycin.

Roxithromycin (**1**) is metabolized[7] to RU39001 (**3**) which retains antimicrobial activity comparable to that of its parent compound *in vivo*. This metabolite derives from **1** by an acidic cleavage of the bond between the macrolide itself and the cladinose sugar. In this case, no ketal formation is possible

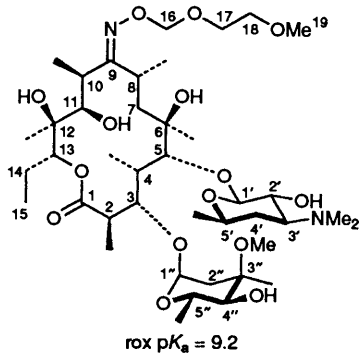

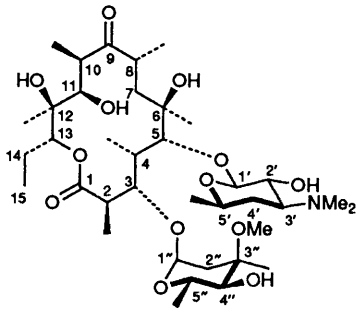

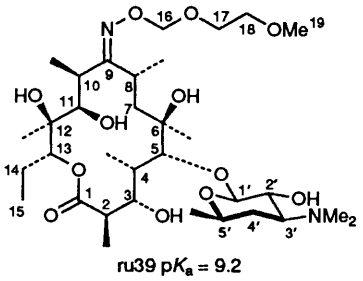

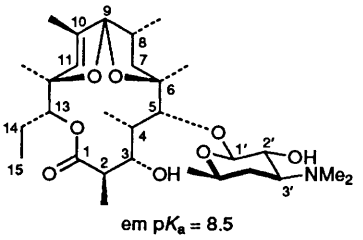

before the loss of the cladinose sugar and the macrolide ring remains intact. Erythromycin A (**2**) is extremely unstable to acid and when administered orally undergoes dehydration *in vivo* leading to an inactive 6,9:9,12-spiroketal metabolite. This occurs *via* translactonization between the 6 and 11-hydroxy groups and the lactone group.[8a] When **2** was allowed to stand in aqueous acid, cleavage of the cladinosyl moiety proceeded gradually with dehydration in the aglycone ring to yield erythralosamine (**4**) which has been reported[8b] as one of metabolites of **2**.

The effects of macrolides on hepatic metabolic enzymes, especially cytochrome P-450, have been studied in order to reduce interference with the metabolism of other drugs.[7] Such effects lead to the induction of cytochrome P-450 and to a stable metabolite–cytochrome P-450 complex after oxidation of the macrolide dimethylamino function. Unlike **2**, **1** has little affinity *in vitro*, with the cytochrome P-450 binding site, and is unable to form significant quantities of P-450 metabolite complex.[9–12] The major metabolite **3** does not form an inhibitory P-450 metabolite complex *in vivo*, and it does not induce hepatic cytochrome P-450. The metabolite of **2**, (**4**) has stronger interaction properties *in vitro* and *in vivo* with the cytochrome P-450 system.[13]

Both drugs **1** and **2** exhibit similar local conformations for their binding and interactions with cytochrome P-450 but their desosamine moiety produces differences in their ability to form stable absorbing (456 nm) cytochrome P-450 metabolite complexes. This is not particularly obvious in the X-ray structures of the two drugs **1** and **2** because in the solid state, only one conformer is observed for these two molecules. Thus, a highly plausible theory may be that their metabolites **3** and **4** are responsible for the cytochrome P-450 activity. These metabolites contain only the binding region. Consequently the selective binding of **4** to cytochrome P-450 and the lack of biological drug interactions for **3** implies that there is a significant proportion of active conformation for **4** and a conformation related to the inhibition of cytochrome P-450 for **3**.

With this in mind, we have initiated a conformational examination of **3** and **4** in solution, using NMR spectroscopy and computational chemical methods (MD). The solution conformation of **1** and its motional properties have been studied by NMR spectroscopy[14] and the use of MD simulation.[15] A reexamination of the conformation of **2** with particular attention given to the active region, required the use of MD and the measurement of heteronuclear coupling constants ($^3J_{CH}$).

The ionization state of the $N(CH_3)_2$ group plays an important role[16a] in the recognition and metabolism of the substrate by the cytochrome P-450. Roxithromycin is only metabolized to the 455 nm absorbing complex at pH 8 or higher[16b] and a fourfold increase is observed for **2** between pH 7.4 and 8.0. RU39001 (**3**), which is the main metabolite of **1**, was unable to form significant amounts of P-450 metabolite complex at all the studied pH values, whereas **4** led to the highest amounts of cytochrome P-450 metabolite complex.

As the protonated macrolides have NMR parameters very similar to those of the unprotonated form, having the crystal structures of **1** and **2**[17,18] one can approximate the other protonated desosamine-containing derivatives and perform a simulation to determine differences in the presence and absence of an NH^+ ion.

Apart from the flexibility of the different units, another feature under investigation by modelling is the persistence in **3** of the hydrogen bonds found in **1**. They could not account for the higher lipid solubility and hence better permeability of **1** and its metabolite through some tissues.[19]

The notation for conformer designation is defined in Table 1 together with some of their characteristics.

Table 1 Notation for conformer designation defined as **A1**, **A2**, **A3**, **B1**, **B2**, **a**, **b**, **c**, **d**, **e**, **I**, **II** and **III**

Torsion angles	(°) of sugar conformations[a]				
	a	**b**	**c**	**d**	**e**
ψ_1	12–20	±5; −15	−30; ±10	15	20
ψ_2	35–45	50–60	−30; 10	55	160
ψ_3	25	35	20	−22	—
ψ_4	45	45	40	−3	—

Macrocycle conformation[b]					
	A1	**A2**	**A3**	**B1**	**B2**
H(2)–H(3)	160	177	165	105–115	145
H(3)–C(1)	40	46	48	3	32
H(4)–H(5)	135	100	140	145–165	165
H(5)–Me(6)	43	55	43	55	−8
H(11)–M e(12)	−73	−76	−63	−76	−58
H(13)–C(1)	−8	14	−20	10	3

Hydrogen-bonding type[c]
Type I: 6-OH–O(16); 12-OH–11-OH; or 6-OH–O(16); 12-OH–11-OH; 11-OH–O-(17)
Type II: 6-OH–O(17); 12-OH–11-OH; or 6-OH–O(17); 12-OH–11-OH; 11-OH–O(17)
Type III: 11-OH–O=C(1); 6-OH–O(16); 12-OH–11-OH; or 11-OH–O=C(1); 12-OH–11-OH; 6-OH–O(16); 6-OH–O(17)
Type: **1**: 3–OH–2′-OH; **2**: 3-OH–O(5′); **3**: 2′-OH–O(5)

[a] The glycosidic dihedral angles: ψ_1, H(5)–C(5)–O(5)–C(1′); ψ_2, C(5)–O(5)–C(1′)–H(1′); ψ_3, H(3)–C(3)–O(3)–C(1″); ψ_4, C(3)–O(3)–C(1″)–H(1″); **a** conformation is characterized by a desosamine orientation nearly perpendicular to the macrocycle; **b** conformation: when the H(3) folds inside the macrocycle, reorientation of the cladinose above the macrocycle and the desosamine rotate with respect to the macrocycle; **c** conformation is characterized by a desosamine sugar coplanar to the macrocycle; **d** conformation: the cladinose orientation is turned back; **e** conformation is characterized by a desosamine sugar coplanar but turned back to the macrocycle. [b] Conformation models **A** and **B** for the aglycones of the 14-membered macrolides: the H(3) to H(5) 'folded-out' type, conformation **A1**; H(5) 'folded-in' type, conformation **A2** and the corresponding H(3) 'folded-in' type, conformation **B1** or **B2**; conformation **A3**: the lactone group C(1)=O, folds inside the macrocycle and allows the 11-OH to form a hydrogen bond with C(1)=O. [c] 6-OH–O(9): Type **I** for **2**; 6-OH–O(9) and 11-OH–O(9): Type **II** for **2**.

Results and Discussion

The X-ray crystal structures of various macrolide antibiotics provide three diamond lattice conformation models (**A**, **B**, **S**) for the aglycone of the 14-membered macrolides.[20–23] The different conformations of the macrocyclic lactone ring generated by MD will later be compared with those found by X-ray analysis (Table S1 of supplementary material).*

* *Supplementary material available.* Table S1, endocycle torsion angles in the X-ray structures and in the MD search. Table S2, experimental ^{13}C and ^1H NMR relaxation times for **1**–**4**. Table S3, complete assignments of all C- and H-signals of the metabolite **3** in $CDCl_3$ at two concentrations (5×10^{-2} and 5×10^{-3} mol dm^{-3}) and in D_2O solution. Table S4, the amplitude, the average and the preponderant values of vicinal proton and some heteronuclear ^1H–^{13}C dihedral angles in the macrocycle for the 100 minimized structures generated. Table S5, the amplitude and the average values of endocycle torsion angles in the macrocycle for the 100 minimized structures generated, protonated and unprotonated. Graph S1, Protocol I (*a*) variation of potential energy *versus* time for minimized structures of **1**, **2** and their metabolites **3** and **4**, (*b*) variation of glycosidic angles ψ_1(H5C5OCl′), ψ_2(C5OCl′H1′), ψ_3(H3C3OCl″) and ψ_4(C3OCl″H1″). Graph S2; Protocol II. Graph S3, Protocol III. Graph S4, Protocol IV.

For details of the Supplementary Publication Scheme, see 'Instructions for Authors,' *J. Chem. Soc., Perkin Trans. 2*, 1993, issue 1 (Supp. Publ. No. 56970, 12pp).

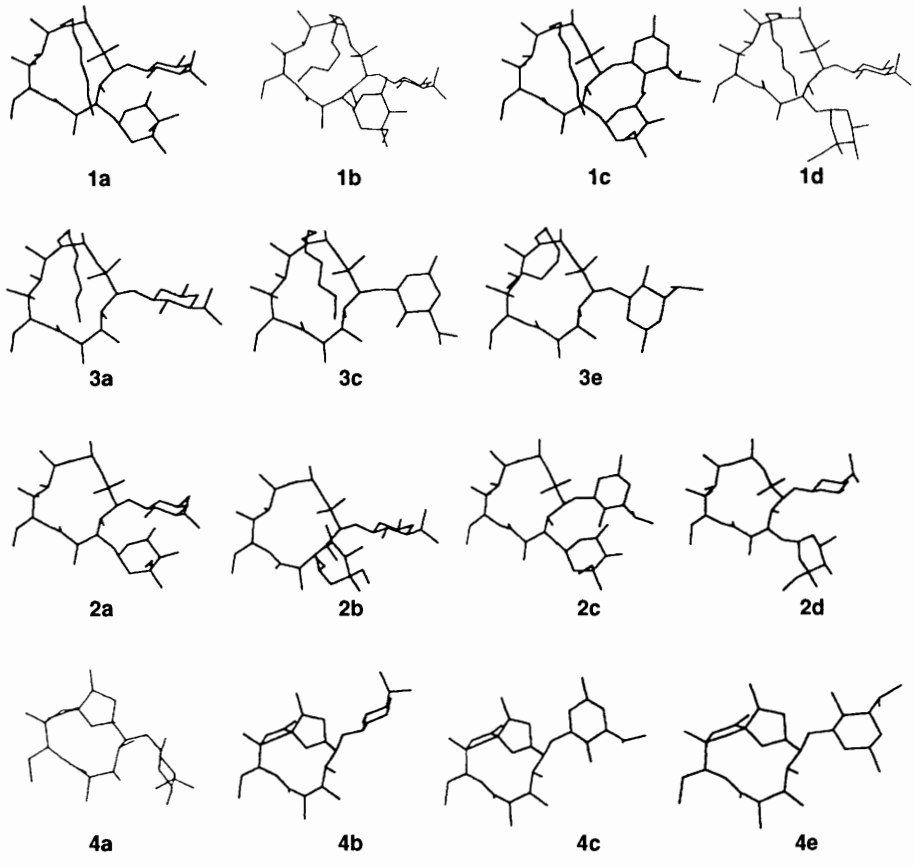

Fig. 1 View of the different structures generated by a systematic conformational search. The four conformers of **1**: **a** (E_p = 66 kcal mol^{-1}, ψ_1 = 16°, ψ_2 = 40°, ψ_3 = 26°, ψ_4 = 47°), **b** (E_p = 72 kcal mol^{-1}, ψ_1 = 14°, ψ_2 = 58°, ψ_3 = 36°, ψ_4 = 42°), **c** (E_p = 68 kcal mol^{-1}, ψ_1 = −25°, ψ_2 = 3°, ψ_3 = 20°, ψ_4 = 40°), **d** (E_p = 72 kcal mol^{-1}, ψ_1 = 15°, ψ_2 = 50°, ψ_3 = −26°, ψ_4 = 4°); and the three conformers of its metabolite **3**: **a** (E_p = 62 kcal mol^{-1}, ψ_1 = 20°, ψ_2 = 45°), **c** (E_p = 60 kcal mol^{-1}, ψ_1 = −8°, ψ_2 = −30°), **e** (E_p = 59.5 kcal mol^{-1}, ψ_1 = 20°, ψ_2 = 160°). The four conformers of **2**: **a** (E_p = 67 kcal mol^{-1}, ψ_1 = 16°, ψ_2 = 40°, ψ_3 = 26°, ψ_4 = 45°), **b** (E_p = 69 kcal mol^{-1}, ψ_1 = 9°, ψ_2 = 60°, ψ_3 = 30°, ψ_4 = 50°), **c** (E_p = 69 kcal mol^{-1}, ψ_1 = −25°, ψ_2 = 5°, ψ_3 = 20°, ψ_4 = 35°), **d** (E_p = 77 kcal mol^{-1}, ψ_1 = 12°, ψ_2 = 50°, ψ_3 = −30°, ψ_4 = 5°), and the four conformers of its metabolite **4**: **a** (E_p = 86 kcal mol^{-1}, ψ_1 = 27°, ψ_2 = 47°), **b** (E_p = 80 kcal mol^{-1}, ψ_1 −15, ψ_2 = 60°), **c** (E_p = 82 kcal mol^{-1}, ψ_1 = −30°, ψ_2 = −20°), **e** (E_p = 83 kcal mol^{-1}, ψ_1 = 5°, ψ_2 = 160°).

The crystal structure of **2** is characterized predominantly by a 'folded-out' conformation **A** (hereinafter named **A1**, Table 1)[20] whereas in the structure **B** (or **B'**) the C(3)–C(5) portion of the macrocyclic ring 'folds inwards' such that H(3) becomes closer to H(11). Thus $\varphi_{C(2)C(3)} \approx -130°$ for **B** (or **B'**), instead of −61° for **A**. However, the similarity in $\varphi_{C(3)C(4)}$ (164.8° and 172.8°) and the $\varphi_{C(4)C(5)}$ (−116.1° and −116.9°) of the two crystal structures, **A** and **B** respectively, implies that the orientation of the sugar rings (conformation **a**) with respect to one another is almost the same for both substances **A** and **B**. The NMR and computational results for **1** presented in previous papers[14,15] illustrate that the molecules in solution or generated during the MD experiment are mainly of **A1** type (low minimized energy). The structures observed by MD confirmed the tendency of the desosamine sugar to adopt a conformation **a** (Fig. 1) with an orientation nearly perpendicular to the macrocyclic lactone ring whereas the two units appear to be in the same plane in a conformation **c** (Fig. 1) only in some protonated structures of **1**. During the MD experiments, the 'higher energy' conformation of the macrocycle is denoted **B1** by analogy to the C(1)–C(3) region in **B** (or **B'**) where $\varphi_{C(2)C(3)} = -128.5°$ and the cladinose sugar moves above the desosamine. The greater discrepancy between the crystal structure **B** (or **B'**) and the observed conformer **B1** occurs especially for the torsion angles C(4)–C(5), $\varphi_{C(4)C(5)} \approx -74°$ for **B1** instead of −117° for **B** (or **B'**). As in the different conformers, the relative orientations of the sugar rings depend on the rotation principally about the C(4)–C(5) and C(5)–C(6) bonds, thus this modification in the **B1** conformation affects the sugar position, assigned as **b** (Fig. 1).

Recently,[22] a hydrogen bridge between OH(11) and O=C(1) has been detected in a crystal structure **S** such that it is observed in the model generated by MD (**A3**) (Table 1). A difference lies in the size of the dihedral angles, C(9)–C(10), C(13)–O(14), which, owing to ring effects, are now reduced to *ca.* 15° (Table S1 of supplementary material). The OH(11) and O=C(1) groups are thus close enough to form a hydrogen bond.

NMR Spectroscopy.—We report detailed NMR results, using ^{1}H and ^{13}C NMR spectra (Table 2), $^3J_{HH}$ values (Table 3) (used to predict solution conformation in $CDCl_3$ solution), ^{1}H nuclear Overhauser enhancement (NOE) (Table 4) and also ^{1}H and ^{13}C relaxation times [available as supplementary material (Table S2) for **3** and **4**]. The complete assignments of all C- and all H-signals of the metabolite **3** in $CDCl_3$ at two concentrations (5×10^{-2} and 5×10^{-3} mol dm^{-3}) and in D_2O solution, by use of the two dimensional techniques are available as supplementary material (Table S3).

Assignments of ^{1}H, ^{13}C NMR signals. The assignments of ^{1}H, ^{13}C NMR signals of **3** and **4** shown in Table 2 are made by a combination of ^{1}H–^{1}H COSY, ^{1}H–^{13}C COSY and ^{1}H–^{13}C long range COSY (COLOC) spectra. Small variations in the chemical shifts (<0.25 ppm) are observed in the desosamine sugar signals at different concentrations in $CDCl_3$

Table 2 ^1H and ^{13}C NMR chemical shifts for **1–4** in $CDCl_3$

	1		**2**		**3**		**4**	
	δ_H	δ_C	δ_H	δ_C	δ_H	δ_C	δ_H	δ_C
Lactone								
1	–	175.2	—	176.3	—	174.8	—	178.4
2	2.88	44.7	2.87	45.0	2.63	44.5	2.72	46.8
2-Me	1.15	16.1	1.18	15.9	1.21	15.3	1.10	13.8
3	3.97	80.1	3.99	80.3	3.52	79.1	4.26	70.1
3-OH	—	—	—	—	3.27	—	3.25	—
4	1.99	38.9	1.97	39.5	2.16	36.7	2.24	44.6
4-Me	1.07	9.1	1.10	9.2	1.05	7.9	1.03	12.6
5	3.51	83.6	3.56	84.0	3.46	92.3	3.41	87.0
6	—	74.9	—	74.8	—	74.4	—	81.9
6-Me	1.47	26.8	1.46	26.4	1.39	25.7	1.40	29.5
6-OH	2.48	—	1.51	—	2.57		—	—
7ax	1.59*	37.4	1.93	38.5	1.61	37.7	2.31	42.9
(isochronous)	1.57							
7eq	1.47*	—	1.74	—	1.32	—	1.60	—
8	3.69	26.9	2.68	44.9	3.74	27.1	2.48	39.9
8-Me	1.01	18.7	1.16	18.4	1.03	18.2	0.92	12.0
9	—	172.8	—	221.9	—	172.4	—	119.7
10	2.64	33.0	3.08	38.1	2.67	33.5	—	139.0
10-Me	1.15	14.7	1.14	14.7	1.18	14.7	1.85	13.8
11	3.80	70.3	3.82	68.8	3.78	70.9	5.50	128.0
11-OH	4.38	—	3.95	—	4.26	—	—	
12	—	74.3	—	74.5	—	74.3	—	88.6
12-OH	3.13	—	3.13	—	3.17	—	—	—
12-Me	1.11	16.2	1.12	16.2	1.17	16.5	1.23	23.0
13	5.07	76.8	5.03	77.1	5.20	76.8	4.94	78.7
14ax	1.45	21.1	1.48	21.2	1.47	21.6	1.59	24.4
14eq	1.88	—	1.91	—	1.92	—	1.35	—
15-Me	0.81	10.6	0.84	10.7	0.81	10.5	0.82	10.2
16	5.15	97.4	—		—	97.6	—	—
δA[a]	5.18	—	—		5.17	—	—	—
δB[a]	5.13	—	—		5.13	—	—	—
17	3.76	68.3	—		—	68.5	—	—
δA[a] (2t)	3.78	—	—		3.74	—	—	—
δB[a] (2t)	3.71	—	—		3.71	—	—	—
18(t)	3.54	71.8	—		—	71.7	—	—
(dd)[a]	3.54	—	—		3.51	—	—	—
19-OMe	3.39	59.0	—		3.37	59.1	—	—
Desosamine								
1′	4.39	103.0	4.40	103.3	4.51	106.5	4.18	104.5
2′	3.22	71.0	3.21	71.1	3.38	70.5	3.19	70.6
2′-OH	3.41	—	3.45	—	3.56	—	3.37	—
3′	2.47	65.5	2.43	63.3	3.15	65.6	2.46	65.4
3′$N(Me)_2$	2.29	40.2	2.29	40.3	2.59	40.2	2.29	40.3
4′ax	1.25	28.8	1.22	29.2	1.36	28.1	1.19	29.1
4′eq	1.67	—	1.67	—	2.01	—	1.60	—
5′	3.46	68.7	3.48	68.8	3.58	70.2	3.48	69.1
5′-Me	1.20	21.3	1.22	21.4	1.24	21.2	1.16	21.2
Cladinose								
1″	4.85	96.1	4.88	96.5	—	—	—	—
2″ax	1.54	35.0	1.56	35.0	—	—	—	—
2″eq	2.34	—	2.35	—	—	—	—	—
3″	—	72.7		72.7	—	—	—	—
3″-Me	1.21	21.5	1.23	21.4	—	—	—	—
3″-OMe	3.28	49.4	3.31	49.5	—	—	—	—
4″	2.99	78.0	3.00	77.9	—	—	—	—
4″-OH	2.20		2.23		—	—	—	—
5″	3.99	65.4	3.99	65.7	—	—	—	—
5″-Me	1.26	18.5	1.27	18.5	—	—	—	—

[a] Values obtained at 400 or 500 MHz.

as in D_2O solution, for **3** (Table S3 of supplementary material).

^{13}C assignments in $CDCl_3$ solution were carried out from the broadband decoupled ^{13}C spectrum, DEPT experiments (90 and 135) (used for multiplicity assignment) and through ^1H, ^{13}C, 2D correlation in its ^1H decoupled version,[24] which confirmed the ^1H chemical shift assignments based on the ^1H 2D COSY experiments. However assignments of two CH groups, CH(3) and CH(5′), were more difficult since their proton chemical shifts were very close (3.49 and 3.50 ppm). Thus the signals at δ 79.1 and 70.2 could be assigned to the two carbons C(3) and C(5′), these carbons were ^1H, ^{13}C long range coupled to Me(2), Me(4) and H(3′), Me(5′) respectively (by way of 2D ^1H, ^{13}C COLOC[25]). Similarly the assignment of

Table 3 Coupling constants (^3J Hz) calculated from **1** and **2** X-ray structures[15] and from the different conformations generated by MD. Vicinal proton–proton coupling constants (^3J in Hz) for **1–4** in $CDCl_3$ solution

	1		**2**		**3**	**4**	J_{calc}				
Vicinal pair	J_{calc}[a]	J_{exp}	J_{calc}[a]	J_{exp}	J_{exp}	J_{exp}	**A1**	**A2**	**A3**	**B1**	**B2**
J_{HH} (Macrocycle)											
2-H, 3-H	11.1	9.9	12.0	9.4	10.5	5.6	10.9	10.8	10.8	2.8	7.9
3-H, 4-H	2.4	1.5	2.3	1.5	1.5	4.0	0.8	0.8	0.9	1.7	2
4-H, 5-H	5.9	7.4	5.3	7.7	2.1	9.0	5.3	2.1	6.5	9.1	7.8
7_{ax}-H, 8-H	11.9	10.5	11.2	11.7	11.1	13	12.4	12.4	12.5	12.5	12.8
7_{eq}-H, 8-H	2.0	3.5	1.3	2.5	2.1	3.2	1.9	1.6	1.8	1.8	5.1
10-H, 11-H	2.4	2.1	1.0	1.3	2.0	1.5[b]	1.2	1.3	0.8	1.6	—
13-H, 14_{ax}-H	11.7	11.2	11.2	11.0	11.2	11.5	11.6	11.6	11.0	11.0	11.3
13-H, 14_{eq}-H	2.4	2.5	1.1	2.4	2.3	3.0	1.6	1.0	1.0	1.0	1.5
J_{CH} (Macrocycle)											
3-H, C-1	2.5	3.3	4.1		s[d] ($W_{\frac{1}{2}}$ = 2.3)	3.5	2	1.9	1.8	5.5	4.1
5-H, C-3	5.3	4.8	5.1	5.8	6.8	2.1	4.9	5.5	5	3.9	2.7
5-H, C_{Me}-6	3	2.5	2.7	3	2.8	2.3	2.6	2.2	2.7	2.1	5.5
13-H, C-1	5.6	3.5[c]	5.5	4	4.2	3.3	5.4	5.3	5.1	5.3	5.6
13-H, C-11	3.7	⩽2[d]	2.9	*f*	1.9	3	2.2	2.5	1.5	2.2	6.4
13-H, C_{Me}-15	2.5	⩽2[d]	2.5	3.2	2.8	3.2	2.3	2.3	2.3	2.4	1.9
J_{HH} (Sugar ring)											
$1'_{ax}$-H, $2'_{ax}$-H	7.7	7.5	7.8	7.2	7.3	7.1					
$2'_{ax}$-H, $3'_{ax}$-H	10.8	10.5	10.5	10.3	10.3	10.0					
$3'_{ax}$-H, $4'_{ax}$-H	12.3	11.2	12.5	12.3	12.5	12.0					
$4'_{ax}$-H, $5'_{ax}$-H	11.3	10.8	11.3	10.8	11.2	*c*					
$1''_{eq}$-H, $2''_{eq}$-H	1.3	1.7	0.9	0.8	—	—					
$4''_{ax}$-H, $5''_{ax}$-H	10.8	9.5	10.9	9.7	—	—					
J_{CH} (Glycosidic bond)							**a**	**b**	**c**	**d**	**e**
5-H, C-1′	5.3	5.2	5.3	5.6	4.7	6	5–5.5	5.2–5.7	4.3–5.4	5.3	5
C-5, 1′-H	2.8	4.5	3.4	2.6	4.6	2.8	3–4	2–3	4–5	2	6
3-H, C-1″	4.4	5.3	4.3	4.0	—	—	4.7	3.8	5	4.8	*g*
C-3, 1″-H	3.1	⩽2[d]	2.7	3.6	—	—	3	3	3.4	5.6	*g*

[a] The calculated $^3J_{HH}$ values for the solid state conformation would be estimated by a Karplus equation of the following type:[14] $^3J_{HH} = (7.8 - \cos\varphi + 5.6\cos 2\varphi)(1 - n\Sigma\Delta Exi)$ and all $^3J_{CH}$ values by a Karplus-type equation of the form:[28] $^3J_{CH} = 5.7\cos^2\varphi - 0.6\cos\varphi + 0.5$. [b] *J* 10-Me, 11-H for erythralosamine. [c] Not determined because of the complexities of the spectra. [d] These signals are detected as singlets (they cannot be correctly estimated because of low resolution). [3] J_{CH} coupling constants < 2 Hz and the corresponding dihedral angles are $50 > \varphi > 120°$ (±). [e] The 2 Hz discrepancy for $^3J_{C\text{-}1,\,13\text{-}H}$ (with respect to the crystal structure or **A1**, **A2**, **A3**, **B1**) is not particularly significant since this coupling constant changes rapidly with small angular changes in this region. However, the main difference could be due to an effect of an electronegativity parameter sensitive to the orientation of the polar lactone group, such as the carbonyl bond, H(13)–C(13)–O(14)–C(1)=O. [f] No signal is detected at the chemical shift of the corresponding ^{13}C. [g] Conformation **e** is only generated by MD for the metabolites **3** and **4** without cladinose sugar.

quaternary carbon is achieved at δ 74.4 for C(6) and 74.3 for C(12), ^1H, ^{13}C long range coupled to Me(6) and Me(12), respectively (by way of 2D ^1H, ^{13}C COLOC).

The configuration of the asymmetric carbon C(3) for the metabolites is assigned by analogy, as the corresponding carbon atom in **1** or **2** would undoubtedly have the same configuration. The absolute configurations of the asymmetric centres in **4** are consistent with those established for **2**. In the NOE difference spectra, a strong NOE is observed between Me(8) and Me(10) which confirms that the stereochemistry of the ethylenic system is '10*Z*' and also the *R* configuration at C(9).

The first observation is that the ^{13}C NMR chemical shifts of **1** and **3** are essentially the same. The single significant variation of the aglycone chemical shifts is a downfield shift at C(5) (+9 ppm) and C(1′) (+3.5 ppm) signals, from **1** to **3**. It is important to assign C(5) unambiguously. This carbon is long range coupled to Me(4) and Me(6) as determined by a 2D ^1H–^{13}C COLOC experiment. This shift could also be caused by a new model **A** (**A2**) involving the C5 portion of the macrocyclic ring or (and) by a different orientation **c** (or **e**) of the desosamine sugar. In the **e** position, the sugar ring is coplanar to the macrocycle with a 'turn back' of 180° relative to the orientation **c**.

The compounds **1–4** differ by the presence or absence of hydroxy groups at C(3). It appears that ^{13}C NMR is useful in assessing intramolecular hydrogen bonding in macrolides.[26] The fact is that the shifts are quite consistent with conformational changes arising from the free hydroxy being tilted (up or down) and hydrogen bonded (or not). Hydrogen bonding to the hydroxy at C(3) will cause the downfield shift of C(3) (+9 ppm). For this reason, the downfield shift of C(3) (+9 ppm) in **3** relative to **4** is most probably due to hydrogen bonding involving the hydroxy at C(3), OH(3)–OH(2′) and OH(3)–O(5′), as observed in the **3** MD results. Since no hydrogen bonding is possible in the derivative **4** as observed in the MD results, the hydroxy group is freer to rotate, and the steric effects of this substituent are felt at the γ carbons. Furthermore, when one compares the ^{13}C NT_1 values from **3** to **4** (Table S2 of supplementary material), they show that in **4**, the hydroxy group is freer to rotate and lessens the rotation of Me(2) and Me(4) to 20 and 50%, respectively.

The temperature dependence of the hydroxy shifts in the two metabolites was investigated (Fig. 2). From this OH(3) essentially is implicated in inter-residue hydrogen bonding in **3** more than in **4**.

Homonuclear $^3J^1H$–^1H and heteronuclear $^3J^{13}C$–^1H coupling *constants*. The determination of $^3J_{HH}$ vicinal proton–proton

Table 4 Qualitative nuclear Overhauser enhancement data for **1**–**4** in $CDCl_3$ solution

	NOE[a]			
^{1}H observed	**1**	**2**	**3**	**4**
3	2 (m), 2-Me (m)	2 (s), 2-Me (s)	2-Me (m)	2 (m)
3-OH			2-Me (m)	
4	2 (m), 3(1)	2 (m), 3 (m)	3 (m)	2 (m), 2-Me (s), 3 (m)
4-Me	2 (m)	2 (m)	2 (l), 3-OH (m)	2 (m), 3 (s)
5	3 (l), 4 (m)	3 (m), 4 (s), 4-Me (s)	3 (s), 4 (s)	3 (m), 4-Me (l)
6-OH	3 (m), 4 (m), 5 (m)		5 (m)	
6-Me	5 (l)		5 (m)	3 (l), 5 (l)
7ax	4 (l), 4-Me (m)		4-Me (m), 6-OH (s)	5 (s)
7eq	6-Me (l)	6-Me (s)		5 (s)
8	6-Me (m), 7 (m)	6-Me (l), 7eq (s)	6-Me (m)	6-Me (l), 7eq (m)
8-Me	7 (m)	7eq (s)	7eq (m), 7ax (s)	7ax (m), 7eq (m)
10	7ax (m), 8-Me (m)	7ax (s)	8-Me (m)	—
10-Me			8-Me (m)	4 (l), 7ax (l), 4-Me (s) 8-Me (l)
11	4 (l), 6-OH (m), 7 (m)	3 (s), 4 (m), 4-Me (m), 7ax (s)	4 (l), 6-OH (l), 7 (m)	7 (m), 10-Me (l)
11-OH			5 (s), 10-Me (m)	—
12-OH	10-Me (m)			—
12-Me	4 (m), 10 (s), 11 (m)	11 (m)	4 (m), 7ax (m), 10 (l), 11 (m)	11 (l)
13	11 (m), 12-OH (m)	11 (m)	11 (m), 12-OH (m)	4 (m), 11 (s), 12-Me (l)
14ax	12-Me (m)	12-Me (m), 13 (s)	12-Me (m)	12-Me (m), 13 (l)
14eq	12-Me (m), 13 (l)	13 (s)	13 (m)	11 (m), 13 (m)
15-Me	2-Me (m), 13 (l)	13 (m), 14 (m)	2-Me (m), 13 (l), 14 (l)	11 (s), 13 (l), 14 (l)
16	11 (s), 11-OH (m)		11 (m), 6-OH (s)	
17	6-OH (m), 6-Me (m)		6-Me (m) 6-OH (m)	
18	3 (m), 6-OH (m), 6-Me (s)		13 (s), 6-Me (m)	
19-OMe	3 (m), 6-OH (s)		2-Me (s), 3 (s), 6-OH (m), 6-Me (s)	
1′	4-Me (m), 5 (l)	4-Me (s), 5 (m)	5 (l), 6-Me (m), 6-OH (s)	4-Me (m), 5 (l)
2′			4-Me (m), 6-Me (m)	6-Me (s), 7ax (s), 10-Me (s)
2′OH			4-Me (s)	4-Me (s)
3-N(Me)$_2$				2′-OH (m)
5′			6-Me (s)	
5′-Me				7eq (m), 5 (s)
1″	2-Me (m), 3 (l)	2-Me (s), 3 (l)		
2″eq	2-Me (s)			
3″-OMe	4-Me (m), 3′ (s), 3′-N(Me) (s)			
5″	5(1), 1′ (s), 5′ (s)	5 (m), 1′ (m), 5′ (s)		
5″-Me	6-Me (s), 19-Me (s), 5′ (s)			

[a] l = large, > 5%, m = medium, > 1%, < 5%, s = small, < 1%.

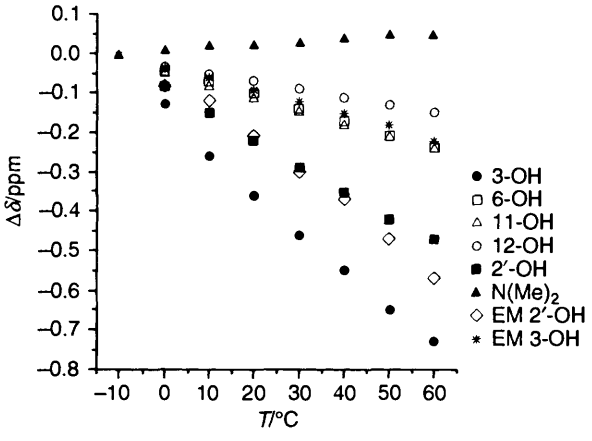

Fig. 2 Temperature effect on the chemical shifts of characteristic protons of the metabolites **3** and **4**: on raising the temperature of the solution (25 to 55 °C), a shift is observed for the lower frequency ($\Delta\delta$ 10^{-2}), for **3**: 3-OH (23) > 2′-OH (20) > 6-OH (12) = 11-OH (12) > 12-OH (7); and, for **4**: 2′-OH (27) > 3-OH (10). On decreasing the temperature of the solution (25 to − 10 °C), a shift is observed for the higher frequency, in almost the same order, 3-OH (50) > 2′-OH (27) > 6-OH (10) = 11-OH (12) > 12-OH (8); and 2′-OH (30) > 3-OH (12), for **3** and **4** respectively. The temperature coefficients ($d\delta/dT$) of **3** and **4** given in the graph for **3**: 3-OH (23) > 2′-OH (20) > 6-OH (12) = 11-OH (12) > 12-OH (7); and for **4**: 2′-OH (27) > 3-OH (10), $-\Delta\delta/\Delta T$ (10^3 ppm K^{-1}).

coupling constants of **3** and **4** shown in Table 3 were made by means of a ^{1}H 2D *J* resolved experiment and by NMR simulation and iteration (PANIC program of Bruker), using the NMR data at 500 MHz.

The conformational analysis of the macrolides is difficult in this case since both conformers differ only in the flexibility of the three units (macrocycle, oxime chain and particularly the desosamine sugar).

(*a*) *Lactone ring conformation.* In solution, the lactone ring of **1** is found to be relatively rigid in the conformation **A1** with the desosamine and cladinose sugar in conformation **a**. The very small values for the small $^3J_{HH}$ coupling constants, $J_{10,11}$ and $J_{3,4}$ and the large $^3J_{HH}$ values for the *trans* coupling constants (Table 3) indicate clearly that the part corresponding to these bonds in the macrocyclic ring of **3**, remains in solution in a similar conformation **A1** as for **1**. But the erythronolide ring region from atoms C(3) to C(6) in **3** does not have the same conformation as **1**. The difference in $J_{4,5}$ [2.1 (**3**), 7.4 Hz (**1**)] is significant with respect to the experimental value for **1**. Compound **1** exists in solution as one major conformer[14] **A1** with φ = 137°, whereas a new model **A2** with φ = 105°, is expected from the solution structure of **3** in which the C(5)–C(7) portion of the macrocyclic ring 'folds inwards' such that H(5) gets closer to H(4). However, the non-similarity in $\varphi_{C(4)C(5)}$ (−97.7, −125.4) and $\varphi_{C(5)C(6)}$ (−77.1, −65.7) of the two structures **1** and **3** respectively (Table S1 of the supplementary material), implies that the orientation of the sugar ring with respect to the macrocycle is not the same for

Table 5 Summary of inter-proton distances (2–3.5 Å) from minimized structures derived from MD at 300 K (p: present, a: absent)

Macrocycle	A1	A2	A3	B1	B2
4–2	p	p	a	p	p
4–2-Me	a	a	a	p	a
5–4	p	p	p	a	a
5–4-Me	a	a	a	p	p
6-Me–3	a	a	a	a	p
7ax–4-Me	a	p	a	a	a
10-Me–8-Me	p	p	a	p	p
10-Me–4-Me	a	a	a	a	p
10-Me–4	a	a	a	a	p
10-Me–7ax	a	a	a	a	p
11–4	p	p	p	a	a
11–3	a	a	a	p	a
11–10-Me	a	a	a	a	p
13–12-Me	a	a	a	a	p
15-Me–2-Me	p	a	a	a	a
Sugar–macrocycle	**a**	**b**	**c**	**d**	**e**
1′–5	p	p	p	p	a
1′–4-Me	p	p	a	p	p
1′–6-Me	a	a	p	a	a
2′–5	a	a	p	a	p
2′–4-Me	a	a	p	a	a
2′–6-Me	a	p	p	a	a
2′–7ax	a	p	a	a	a
2′–10-Me	a	p	a	a	a
5′–4-Me	a	a	a	a	p
5′–6-Me	a	a	p	a	a
5′-Me–3	a	a	a	a	p
5′-Me–5	a	a	a	p	a
5′-Me–6-Me	p	a	p	a	a
5′-Me–7e	a	p	a	a	a
1″–3	p	p	p	p	a
1″–2-Me	p	p	p	a	a
1″–5	a	a	a	p	a
2″–2-Me	p	a	p	p	a
3″-OMe–2-Me	a	a	a	p	a
3″-OMe–4-Me	p	p	p	a	a
5″–5	p	p	p	a	a
5″–4-Me	a	a	a	p	a
5″–6-Me	a	p	a	a	a
5″-Me–6-Me	p	a	p	a	a
Inter-sugar	**a**	**b**	**c**	**d**	**e**
3″-OMe–1′	p	p	a	a	a
3″-OMe–3′	p	a	a	a	a
3″-OMe–5′	a	p	a	a	a
3″-OMe–N(Me)$_2$	p	a	a	a	a
5″–1′	p	a	p	a	a
5″–5′	p	a	a	a	a
5″-Me–1′	a	a	p	p	a
5″-Me–3′	a	a	p	p	a
5″-Me–5′	p	a	a	p	a

both substances: conformation **a** for **1**, predominantly **c** and **e** for **3**.

Even the erythronolide ring for atoms C(6) to O(14) and perhaps the sugar ring (desosamine) do not have the same conformation in **4** as in **2**. The C(1) to C(6) region is reorganized with respect to the conformer **2**, especially the low value of $^3J_{2,3}$ [5.6 (**4**), 9.4 Hz (**2**)] which in this case indicates conformational deformation around the C(2)–C(3) bond (Table 3). The 'folded-in' model **B** is characterized by $^3J_{2,3}$ = 6.6 Hz.[20] Further large changes are observed in the comparison between J_{exp} **2** and **4**: $^3J_{3,4}$ = 1.5 (**2**) and 4.0 Hz (**4**); $^3J_{4,5}$ = 7.7 (**2**) and 9.0 Hz (**4**).

The solution of **2** is characterized predominantly by conformation **A1** although the possibility of a conformational equilibrium with the model **B1** has been noted by the MD study. In the structure of **4** a major model **B2** (approximately consistent with the model **B1**) was considered with the C(3) carbon of the macrocyclic ring 'folded inwards' such that H(3) gets closer to H(2). However, the non-similarity in the torsion angles $\varphi_{C(2)C(3)}$, $\varphi_{C(3)C(4)}$, $\varphi_{C(4)C(5)}$ (Table S1 of the supplementary material) and the presence of double bond C(10)=C(11) affects conformer **B1** in these regions. Finally, the non-similarity in the torsion angles $\varphi_{C(3)C(4)}$ (164.8°, 142.8°) and $\varphi_{C(4)C(5)}$ (−116.1°, −70.8°) of the two structures, **2** and its metabolite, implies that the orientation of the sugar rings with respect to one another is not the same for both substances, conformation **a** for **2** and **b** for **4**.

All these novel conclusions will be further tested using molecular dynamics experiments. Determination of heteronuclear ^{13}C–^1H coupling constants by selective 2D INEPT[27] is a useful experiment in this case since both conformers differ only in the flexibility of C(3) and C(5) of the macrocyclic ring in the structures **B** and **A2**, respectively. The values of $^3J_{CH}$ (Table 3) measured for the macrocycle in **3** and **4** are similar to those predicted for **A2** and **B2**; $^3J_{C(1)H(3)} \approx 2$ (**3**), 3.5 (**4**), 1.9 (**A2**), 4.1 (**B2**) and $^3J_{C(3)H(5)} \approx 6.8$ (**3**), 2.1 (**4**), 5.5 (**A2**), 2.7 (**B2**).

(*b*) *Sugar ring conformation.* The different positions of sugar moieties **a**, **b**, **c**, **d**, **e** appear in Fig. 1 and their characteristics are reported in Table 1. Determination of the heteronuclear ^{13}C–^1H coupling constants by selective 2D INEPT experiments is especially helpful for glycosidic bonds in order to find the relative positions of the sugar moieties towards the erythronolide. The selective excitation of the macrocycle protons H(3) [for $\psi 3$, H(3)C(3)O(3)C(1″)] and H(5) [for $\psi 1$, H(5)C(5)O(5)C(1′)], and selective excitation of the sugar protons H(1′) [for $\psi 2$, C(5)O(5)C(1′)H(1′)] and H(1″) [for $\psi 4$, C(3)O(3)C(1″)H(1″)] led to the $^3J_{CH}$ values presented in Table 3. The data do not support a single conformation model for the sugar rings and only conformational averaging can give good agreement between theoretical (MD) and experimental NMR data.

The torsion angles, ψ_1 and ψ_2 of generated structures can be correlated, by using a Karplus-type equation[28] (for the C–O–C–H segment), to corresponding coupling constants. Thus, our observed values for $^3J_{C(1')H(5)}$ and $^3J_{C(5)H(1')}$ can be compared to those of minimized structures, generated by an MD study *versus* the different protocols (Table 3): for the metabolite **3**, $^3J_{H(5)C(1')}$ = 4.7 and $^3J_{C(5)H(1')}$ 4.6 Hz, there should be greater participation of conformer **c** with **a** and **e**; for **2**, $^3J_{H(5)C(1')}$ = 5.6 and $^3J_{C(5)H(1')}$ = 2.7 Hz there is predominantly conformation **a** in equilibrium with the model **B1b** as noted by the MD study describing an average of **a**, **b**, and **c**. Its metabolite **4** with $^3J_{C(1')H(5)}$ = 6.0 and $^3J_{C(5)H(1')}$ = 2.8 Hz becomes predominantly form **b** with little participation of conformations **c** and **e**.

Nuclear Overhauser enhancement (NOE) experiments. 2D Phase-sensitive ^1H NOESY experiments in $CDCl_3$ were performed using a time-proportional phase-increment method.[29] The observed NOE values in Table 4 are compared with the spatial proximity values computed from the low-energy conformers having sugars in **a**, **b**, **c**, **d**, **e** positions in Table 5. Differences from macrolides were observed for some NOEs, particularly those from H(11) such as [11]4 expected for models **A** but [11]3 and [11]10Me only observed for conformers **B1** and **B2** respectively. The very small NOE [11]3 and [4Me]5 which appears only in models **B** are observed for **2**; they could be due to a minor conformer **B1** in equilibrium with the major one **A1**. In the same way, the large NOEs [10Me]4, [10Me]7ax, [11] 10Me, [6Me]3 observed for **4**, as NOE [14eq] 11, characterize and confirm the **B2** conformation for **4**. Moreover the particular conformation **b** of the desosamine sugar for **4** is confirmed by the

Table 6 The different conformational parameters of each unit in minimized structures for **1–4** protonated and unprotonated. Potential energy of minimized structures with their statistical participation (in %) *versus* the different protocols

	Macrocycle conformation					Sugar conformation				
E_p/kcal	**A1**	**A2**	**A3**	**B1**	**B2**	**a**	**b**	**c**	**d**	**e**
Protocol 1										
1	100	—	—	—	—	90	—	10	—	—
66	(50)					(50)		—		
70/75	(50)					(40)		(10)		
2	50	—	40	10		50	10	40	—	—
67/69	(40)		(30)	(10)		(40)	(10)	(30)		
70/75	(10)	—	(10)	—		(10)		(10)		
3	30	50	20	—		30	—	40	—	30
64/67	(20)	(40)	(20			20		(30)		(30)
67/70	(10)	(10)	—			(10)		(10)		—
4		20	—	—	80	—	80	—	—	20
80/82		—			(80)		(80)			—
87		(20)			—		—			(20)
Protocol 2										
1	90	—	3	7	—	50	7	18	25	—
67/69	(25)		—	—		(15)	—	(10)	—	
70/75	(65)		(3)	(7)		(35)	(7)	(8)	(25)	
2	50	—	40	10	—	62	10	20	**8**	—
67/69	(30)		(30)	—		(47)	—	(13)	—	
70/75	(20)		(10)	(10)		(15)	(10)	(7)	(8)	
3	20	75	5	—		77	—	23	—	—
60/63	(13)	(38)	—			(35)		(16)		
64/68	(7)	(37)	(5)			(42)		(7)		
4	—	64	—	—	36	64	36	—	—	—
80/82		—			(36)	—	(36)			
86/88		(64)			—	(64)				
Protocol 3										
1	86	—	9	5	—	95	5	—	—	—
66/68	(55)	—	(5)	—		(60)	—			
68/70	(20)	—	(2)	—		(22)	—			
70/74	(11)	—	(2)	(5)		(13)	(5)			
2	80	—	17	3	—	92	3	5	—	—
67/68	(71)		(11)	—		(82)	—	—		
68/71	(9)		(6)	(3)		(10)	(3)	(5)		
3	54	43	3	—	—	53	—	42	—	5
59/61	(25)	(14)	(1)			(2)		(36)		(2)
61/63	(25)	(20)	—			(38)		(6)		(1)
63/68	(4)	(9)	(2)			(13)				(2)
4	—	—	—	—	100	—	90	8	—	2
80/83					(95)		(87)	(6)		(2)
83/85					(5)		(3)	(2)		—
Protocol 4										
1 (prot)	86	—	13	1	—	75	1	24	—	—
90/92	(66)	—	(2)	—		(59)	—	(9)		
92/94	(15)	—	(7)	—		(11)	—	(11)		
94/96	(5)	—	(4)	(1)		(5)	(1)	(4)		
2 (prot)	77	—	19	4	—	77	4	19	—	—
92/93	(75)		(18)	—		(75)	—	(18)		
93/94	(2)		(1)	(4)		(2)	(4)	(1)		
3 (prot)	43		10	—	—	48	—	52	—	—
61/63	(30)	47	—			(20)		(40)		
63/68	(13)	(30)	(10)			(28)		(12)		
4 (prot)	—	(17)	—	—	100	—	92	8	—	—
106/107					(92)		(92)	—		
107/109					(8)		—	(8)		

characteristic spatial proximity between H(2′) and Me(6), H(7a) and Me(10).

For **1** and **3**, the phase sensitive 2D ^{1}H NOESY in $CDCl_3$ (Table 4) demonstrated that the oxime chain is directed between C(8) and OH(11) towards Me(6) and OH(6). This reduces the degree of freedom of the macrocyclic lactone ring which corresponds to conformation **A** only. In molecule **3**, the desosamine sugar makes an '**a**↔**c**' interconversion; three desosamine–lactone NOEs, particularly those from Me(6) were observed, corresponding to an interaction between the macrocycle and conformation **c** which is nearly coplanar to the lactone ring, [1′]Me(6), [2′]Me(6) and [5′]Me(6). In the **Ac** or **Ae** conformation, the oxime chain is repelled above the macrocyclic lactone ring towards the carbonyl group C(1)=O; a characteristic spatial proximity between H(18) and H(13) is found in this metabolite **3**. The medium NOE[11]Me(4) only observed for **3**, allows us to conclude that this unexpected NOE could be due to the presence of conformer **A2**, perhaps in

equilibrium with **A1** and **A3**. Some interesting intra-residue NOEs from model **A3** were observed for **3**, particularly those from Me(12) such as [Me(12)]4 and [Me(12)]7a.

^{13}C Spin-lattice relaxation times (T_1). ^{13}C NMR relaxation measurements (T_1 data) led to the same conclusions as the NOE data, with respect to the conformation in solution. T_1 values were used to probe the mobility of the protonated carbons in **1**–**4**. Information about the structural flexibility of these compounds can be obtained experimentally from the T_1 relaxation times of the carbon resonances as the NT_1 values (N = number of attached protons, T_1 = longitudinal relaxation time) correlate directly with the molecular mobility.[30]

The presence of the oxime moiety on one side in metabolite **3** reduces the mobility of this part of macrocyclic lactone ring and is in good agreement with the amplitude of torsion angles in the C(6)–C(13) region ($\leqslant 5°$ for **3**) observed during the MD (Tables S4, S5 and Graph S1 of the supplementary material). Consequently the motion of the desosamine sugar on the opposite side is liberated. The [ΔT_1C of NMe_2] shows that the desosamine sugar is more mobile in **3** (average of conformations **a**, **c** and **e**) than in **1**, +48% and also than in **2** and **4**, $\approx +20\%$, respectively. The amplitudes of torsion angles of the desosamine moiety during a 100 ps simulation, ψ_1 (59°), ψ_2 (160°), are different for **3** with respect to **1**, ψ_1 (9°) and ψ_2 (17°). As for the macrocycle, the ^{13}C NT_1 values for the flexible side chain were small. This result was indicative of the contribution of the oxime chain conformation that restricted its rotation and is in agreement with the existence of a hydrogen bond network between the oxime chain and the macrolactone. The hydrophobic face of **3** leads to more steric hindrance for all the methyl groups. The small T_1 values for 6-Me, 8-Me, 10-Me, 12-Me and 15-Me compared with **2** and **4** were indicative of sterically hindered rotation. Moreover, this provides better access to hydroxy protons on the other face to bind to the oxime chain by hydrogen bonding. Indeed conformation **A** is characterized by a very high calculated energy barrier to rotation of Me(2), however, the inward folding of the lactone ring in model **B** removes the steric hindrance to rotation of Me(2) and the calculated energy barrier drops by a factor of ≈ 5. In good agreement with the literature,[24b] the ^{13}C T_1 values of **4** relative to that of **2** are increased by +108% for Me(2) and decreased by −20% for Me(4). By contrast in **3**, the loss of the cladinose sugar reduces energy barriers to the rotation of Me(2) and also of Me(4), relative to that of **1** (+85% and +15% for the ^{13}C T_1, respectively, (Table S2 of supplementary material).

Molecular Dynamics.—We performed computational chemical calculations (molecular dynamics and molecular mechanics calculations), starting with the X-ray crystal structure of **1**[17] for **1** and **3** and the X-ray structure of **2** from the Cambridge Data Bank[18] for **2** and **4**. The final structures obtained after several such calculations were examined for the overall energetic favourability and compared with the structure derived from the NMR data. The aims of this work are to use MD calculations: (i) to determine the flexibility of the sugar rings about the glycosidic bonds joining the sugars to the lactone ring and predict the available conformational space for desosamine; (ii) to determine the rotational freedom about the endocyclic dihedral angles in the macrocycle and thus, on the basis of the minimum energy level of the conformation **A**, to generate the approximate ratios of minimum-energy conformations available up to 1–3 kcal mol^{-1}.* Structures found to have more energy, up to 10 kcal mol^{-1} are representative of very hindered intermediates.

* 1 cal = 4.184 J.

Table 3 compares the NMR data with the resulting dihedral angles for all different conformations obtained from MD. The similarity between the geometry in solution and several MD conformers was also investigated from the intensive NOESY correlations observed (Tables 4, 5). In Table S4 and S5 (available as supplementary material) we have reported the amplitude and the average values of endocyclic torsion angles and vicinal proton and some heteronuclear ^1H–^{13}C dihedral angles for the macrocycle, for the 100 minimized structures generated. Table 6 summarizes the exploration of conformational space covered during the simulations (potential energy and statistical participation of every conformation).

Preliminary Protocols.—The MD simulations were carried out using the 'DISCOVER' program of BIOSYM package[31] on a Silicon-Graphics 4D-35G computer. The X-ray structures of **1** and **2** were used to build the molecular structure and topology for **3** and **4** respectively, with removal conversion of the cladinose sugar by a hydroxy group, and for their protonated derivatives, with the desosamine sugar modified in the protonated amino functional group. The starting coordinates of **2** were used as the starting conformation for the simulation of the metabolite **4** with removal conversion of the 6- and 11-OH groups and the lactone group by a 6,9:9,12-spiroketal. Therefore, to create the starting structure for **4** we chose to force the torsions H(2)C(2)–C(3)H(3) and H(4)C(4)–C(5)H(5) to the values found in the NMR solution, 125° and 160° respectively, while all other torsions are not forced. These values were then introduced using a relatively high force constant of 15 kcal mol^{-1} (35 kcal mol^{-1} proved too high), and the system was allowed to come to equilibrium for 4 ps. The atomic velocities are randomly applied following a Boltzmann distribution to obtain a temperature of 900 K for simulated-annealing (Fig. 3). The temperature was further reduced to 300 K by different steps during 50 ps (700 and 500 K). The torsion force constant was then suppressed and the simulations made at 300 K during 50 ps. The macrocycle was fixed in the **B2** geometry as also found by NMR in the solution-state conformation, the motion of erythronolide being very restricted.

The starting structures of the molecules **3** and **4** have the disadvantage of not having X-ray information available. Another technique used for generating the structures may include conformational systematic searches by rotation of torsion angles (Fig. 3). This empirical method allowed us to verify whether the sampling of the conformational space was complete during the MD calculations. We exclude from consideration all conformers that have total energies of more than 10 kcal mol^{-1} greater than the lowest energy conformer. The stable conformers **a**, **c** and **e** for **3** and **b**, **c** and **e** for **4** were obtained from the energy maps calculated by the rotation of ψ_1 and ψ_2 per 5°. Combined incrementation of the glycosidic bonds ψ_1 and ψ_2 was performed with a minimization step after each increment. For each increment of ψ_1, ψ_2 was incremented 72 times for a complete rotation and so on for each of the 72 values of ψ_1. The minimization consisted of a single iteration of the steepest descent algorithm in order to measure the potential energy at each position. The available low-energy conformers were also reproduced after simulated-annealing (Fig. 3) or a detailed modelling procedure described in an earlier paper.[15]

Protocol I. (Graph S1 of the supplementary material). For a preliminary conformational exploration, after energy minimization and an equilibration period, we performed for **1**–**4** a 40 ps MD run at 300 K with periodic temperature jumps to 600 K to supply the system with energy (to pass conformational barriers) (Fig. 3). The simulation was stopped every 4 ps and the remaining structure energy minimized. In this case, we performed the molecular dynamics calculations starting with X-ray structures of **1** for

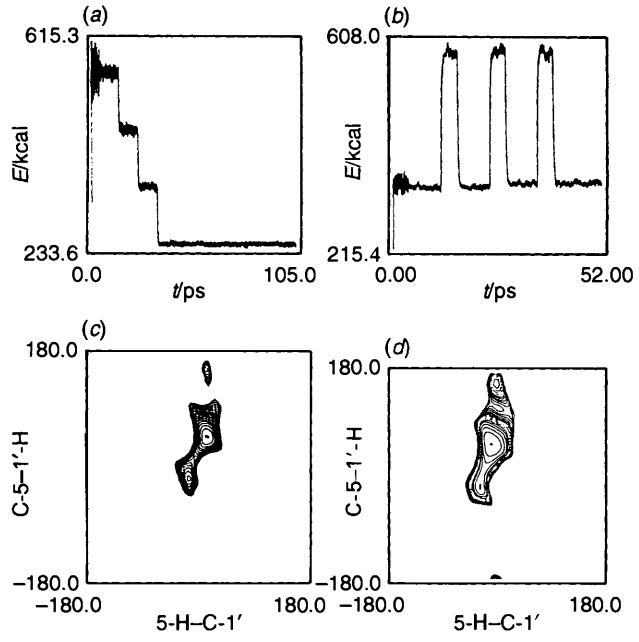

Fig. 3 Preliminary conformational exploration. The technique of conformational systematic searches used for generating a collection of 'significant' conformers may include, (*a*) simulated-annealing, a temperature of 900 K is then reduced to 300 K by different steps during 50 ps (700 and 500 K). The torsion force constant is then suppressed and the simulations are made at 300 K during 50 ps; (*b*) a 40 ps MD run at 300 K with periodic temperature jumps to 600 K; (*c*) iso-energy map of **3** and (*d*) the erythralosamine (**4**) molecule as a function of the ψ_1 [H(5)C(5)O(5)C(1′)] and ψ_2 [C(5)O(5)C(1′)H(1′)] torsion angles. In all cases, iso-energy contours are drawn at increments of 1 kcal mol^{-1} with respect to the absolute minimum. The drawings of the three low-energy conformers referred to ψ_1 and ψ_2 values on maps 5*c* and 5*d* are shown in Fig. 3 and correspond to three conformers of the metabolite **3**: **a** (E_p = 62 kcal mol^{-1}, ψ_1 = 20°, ψ_2 = 45°), **c** (E_p = 60 kcal mol^{-1}, ψ_1 = −8°, ψ_2 = −30°), **e** (E_p = 59.5 kcal mol^{-1}, ψ_1 = 20°, ψ_2 = 160°) and three conformers of the metabolite **4**: **b** (E_p = 80 kcal mol^{-1}, ψ_1 = −15°, ψ_2 = 60°), **c** (E_p = 82 kcal mol^{-1}, ψ_1 = −30°, ψ_2 = −20°), **e** (E_p = 83 kcal mol^{-1}, ψ_1 = 5°, ψ_2 = 160°).

1 and **3**, and of **2** for **2** and **4**, without applying the distance or the dihedral angles constraints obtained from the NMR experiments.

Molecules **1** of lowest energies generated during this experiment are only of **Aa** type. In this protocol, its metabolite **3** exhibits both **A1**, **A2** and **A3** with population of the sugar **a**, **c** and **e** in the same ratio. The **e** position is stabilized by hydrogen bonding involving O(5′), [3-OH–O(5′)] while [3-OH–OH-2′] stabilizes position **c**. The average structure from MD is more stable by 2 kcal than one issue of **1** and the more flexible desosamine sugar gives large fluctuations corresponding to its different conformations.

Molecules (**2**) of lowest energies generated during this experiment are mainly of **A** conformation, **A1** and **A3**, involving as much perpendicular sugar ring orientation **a** as planar desosamine ring **c**. This **A**-type conformation is in equilibrium with the remaining **B1b** conformation which is in the same energy range. This experiment provides an important confirmation that **2** is best described as having the overall minimum energy structures **A1**↔**A3**↔**B1** and the three different positions of sugar moieties **a**↔**b**↔**c**. The minimum energy structure of its metabolite **4** is predominantly **B2** with an orientation **b** of the desosamine sugar perpendicular to, and above the macrocycle (Fig. 1). The minor conformation of this molecule corresponds to a conformation **A2e** of 'higher energy' (5 kcal above the minimum).

Protocol II. (Graph S2 of the supplementary material). To locate other stable contributing conformations, the 40 ps trajectory was sampled every picosecond, and the structures were then minimized by molecular mechanics and stored.

With protocol II, we have generated for **1** and **2**, one conformation of 'higher energy'—**Ad** with a 'turned-back' cladinose (5 kcal above the minimum). This structure does not appear in the first protocol and would participate to a small extent in erythromycin conformation. The deviations from the X-ray structure are essentially ψ_3 (Δ = −56°) and ψ_4 (Δ = −45°) (Fig. 1). The main difference between the two macrolides **1** and **2** is that the conformations **Ad** and **B1** are probable in solution for **2** but improbable for **1**.[15] With this protocol, we have generated for **2** three located stable macrocycle conformations **A1**, **A3**, **B1** and four corresponding desosamine orientations **a**, **b**, **c** and **d**. Its metabolite is less flexible and always presents the major conformation **B2b**, this time accompanied by the **A2a** conformation of 'higher energy' (6 kcal above the minimum).

Protocol III. (Graph S3 of the supplementary material). The stability of the different conformers of **1**–**4** has been tested by a protocol without raising of the temperature (300 K) but using a long time scale (100 ps) with energy minimization every 1 ps (Table 6). Molecules **1** and **2** of lowest energies, generated during this experiment are mainly of **A** type (**A1** and **A3**). This **Aa**-type conformation is in equilibrium for **2** with two conformations of intermediate energies such as **B1b** and **Ac**. However for **1** this experiment provides little **B1b** conformation of higher energy. For one metabolite **4**, the conformation **B2b** becomes the major structure with the remaining of **B2c** and **B2e** conformations. For the other metabolite **3**, the most important conformations of minimum energy are the model **Ac** with a parallel positioning of desosamine and macrocycle moieties and the model **Aa** with the sugar ring perpendicular to the macrocycle (**A1** and **A2**). **Ae** contributes only slightly to the other stable conformations.

The evolution of the models at 300 K shows different energies according to the type of hydrogen bonding. Both compounds **1** and **3** are stabilized by the relatively strong inter-residue hydrogen bond (chain–macrocycle), enhanced for **3** by the addition of 3-OH–OH-2′ and 3-OH–O(5′) stabilizing conformations **c** and **e**, respectively. This induces the presence of an intramolecular hydrogen bond network in the macrocycle between the oxime chain and the desosamine residues, while hydrogen bonding in the macrocycle residue of **2** is weak and non-existent in **4**.

Structures **1**, **2** and **3** present some conformations **A3** characterized by the hydrogen bonding 11-OH–O=C(1).

If we analyse the amplitude of the movement of the endocyclic torsion angles in the macrocycle for **1** and **2** (illustrated in Fig. 4), the greatest deviation (61°) is observed for the C(2)–C(3) dihedral angle, with smaller effects on the neighbouring C(4)–C(5) (≈26°) and C(5)–C(6) (≈18°). This motion is only observed for **1**; **2** generates the **B1** type conformation. For **3**, an attenuation (of 53°) of the endocyclic torsion angles' amplitude can be noticed in the C(2)–C(3) region as conformation type **B** does not exist for **3** (Table S5 of supplementary material). However, we find a high amplitude for the endocyclic torsion angle C(4)–C(5) (37°). This induces the different conformation **A2** of this macrocycle. For the metabolite **4**, no amplitude of any of these torsion angles implies no possibility of interconversion with any **A** conformation and only one rigid conformation **B2** is observed. The amplitude of movement of the ethyl group leads to two positions, parallel and perpendicular to the macrocycle, only for the metabolites **3** and **4**. We observed a slight rotation of the two glycosidic bonds, ψ_1 and ψ_2, only for **1** (**1** is best described as a major conformer **a**), whereas a larger rotation of these angles arose for **2**, involving greater mobility of the sugar moieties **a**, **b**, **c** (and **d**) positions. The most important variations of the dihedral angles

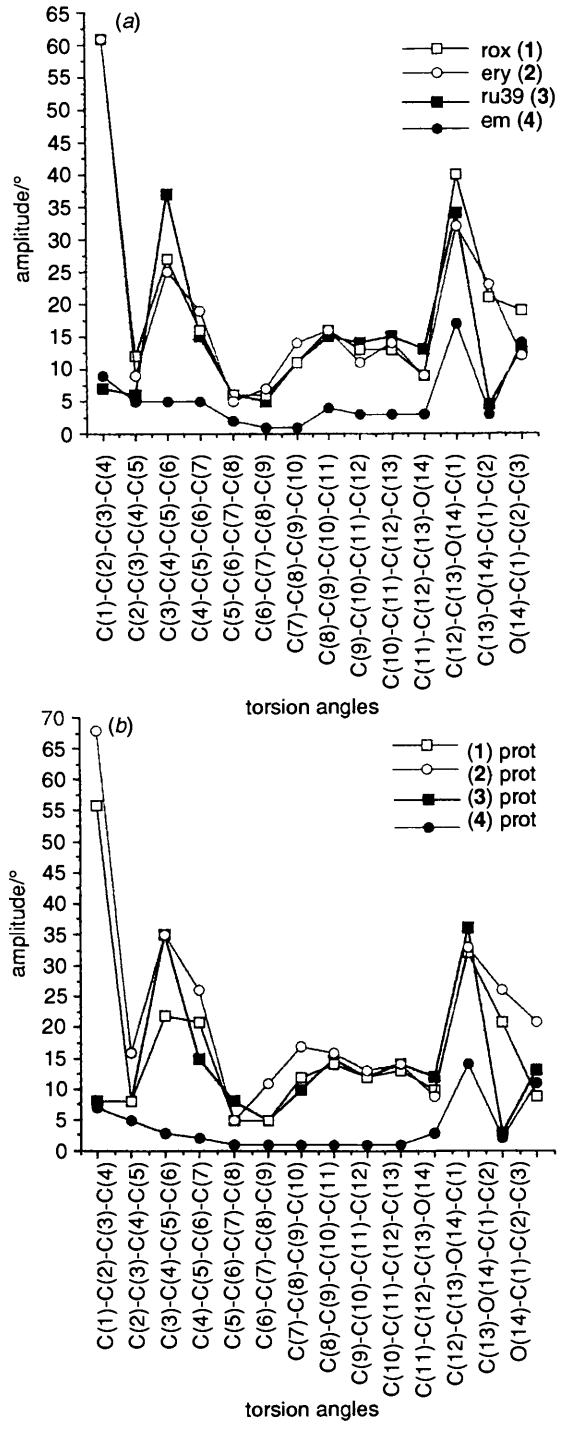

Fig. 4 Amplitude of endocycle torsion angles for (*a*) **1–4** and (*b*) for protonated derivatives, respectively (MD at 300 K)

for **3** and **4**, compared with the parent molecules, affect the glycosidic bonds, ψ_1 and ψ_2. This induces conformation **e** ($\psi_1 = +20°$, $\psi_2 = +160°$) which is not represented in the generated parent molecules and conformation **c** ($\psi_1 = -25°$, $\psi_2 = +10°$) which participates significantly for the metabolite **3** but weakly in the case of **4**.

Protocol IV. (Graph S4 of the supplementary material) (for the protonated derivatives). The ionization state of the dimethylamino functional group of the desosamine sugar was taken into account in order to check the eventual consequences on conformational properties according to the electrostatic term. We performed 100 ps of MD at 300 K (as described in protocol III).

Analysis of the 100 minimized structures generated highlighted the three different conformations for the sugar rings **a**, **b**, **c** and the macrocycle conformations **A** and **B** (Table 6). During the simulation, two new hydrogen bonds appeared in 100% of the generated structures, (3′) $N(Me)_2H^+$–OH(2′) and (2′)OH–O(5), in addition to the different types of hydrogen bonding already existing (**I**, **II**, **III** and **1**, **2**, **3** Table 1).

A combination of minimum potential-energy structures of conformations **Aa**, and conformation **Ac**, 3 kcal above the minima, appear to contribute to produce a stable protonated solution conformation for **1–3** respectively. The **b** conformation is taken into account only for erythromycin (**B1b**) and above all for its derivative (**B2b**). No conformation **e** is induced with this protocol.

In Fig. 4 a large amplitude is observed in the C(12)–C(1) region as the **A3** conformation increases during this protocol in all the compounds **1–3** (particularly for **3**) while the conformations **A1** or **A2** have the same participation. On the other hand, conformation **B** is practically non-existent for **1** and its metabolite, but the contribution remains the same for **2** and its derivative.

The mobility around the glycosidic bonds, ψ_1 and ψ_2, is sufficient to increase significantly the coplanar conformation **c** in the generated structures **1–3** of this experiment (but not for **4**). This corresponds to the most important variation compared with the unprotonated molecules. At the same time the other coplanar conformation **e** disappears for the metabolites **3** and **4**. We noted for metabolite **4** no modifications between the protonated and the unprotonated molecule.

Conclusions

The detailed modelling procedure described in a former paper [15] provided support for the conformational study of these macrolide derivatives. The different protocols for the MD simulations have been used to generate many different structures and to explore fully the conformational space of these compounds. At the same time, a detailed examination of the NMR data revealed that approximate solution structures can be estimated. Therefore, we can postulate a reasonable solution structure for these compounds and their protonated analogues (Fig. 5).

A combination of NMR spectroscopy and MD shows that the conformations in solution of the major metabolites **3** and **4** possess a lactone ring reorganized in the C(3)–C(5) region in the models **A2** or **B2** respectively. At the same time, this macrocycle flexibility induces five different orientations, **a**, **b**, **c**, **d** and **e** for the desosamine sugar. In **1**, the desosamine sugar adopts a conformation **a** with an orientation nearly perpendicular to the macrocyclic lactone ring whereas in **3** the two units seem to be in the same plane with conformations **c** and **e**. For **2**, the major conformations **a** and **c** are in fast exchange with a minor conformation **b** with the sugar ring lifted above the macrocycle but this slight participation increases significantly for its metabolite **4**. The conformation **b** is unlikely for the two products **1** and **3**.

The main conformations of the protonated derivatives **1–3** are essentially the **Ac** and **Aa** conformations (**A1**, **A2** or **A3**). In the case of protonated **2** there is also a slight participation of **B1b** while its metabolite **4** is always represented essentially by the conformation **B2b**; conformation **c** is favoured over the **a**, **b** or **e** one (this last has totally disappeared). Both compounds **1** and its metabolite **3** are stabilized by the relatively strong inter-residue hydrogen bond (chain–macrocycle) strengthened for **3** by a new inter-residue hydrogen bond (desosamine–macrocycle), 3-OH–OH-2′ and 3-OH–O(5′) which stabilize conformations **c** and **e** respectively. This induces the presence of an intramolecular hydrogen bond network in the **1** and **3** macrocycle between the oxime chain and the desosamine

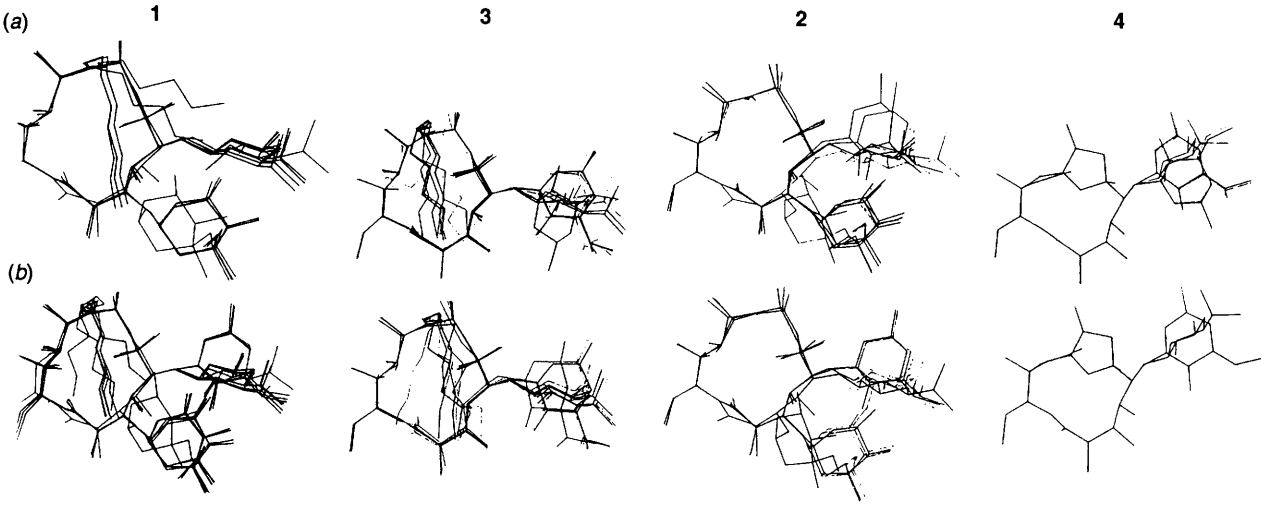

Fig. 5 Conformational averaging (*a*) for roxithromycin (**1**), structures **A1aI**, **A1aII**, **A3aIII** and **B1bI**: its metabolite **3**, structures **A1aII**, **A1cII1**, **A2cI1**, **A2cII1**, **A3III1**, **A1eII2**, **A2eII2**; **2**, structures **A1aII**, **A3aIII**, **A1cII** and **B1bI**; its metabolite **4**, structures **B2b**, **B2c** and **B2e**; and (*b*) for their protonated derivatives: **1**, structures **AaI**, **AaII**, **AaIII**, **AcI** and **BbI**; its metabolite **3**, structures **A1aII**, **A1cII1**, **A2cI1**, **A2cII1**, **A3cIII1**; **2**, structures **A1aII**, **A3aIII**, **A1cII** and **B1bI**; its metabolite **4**, structures **B2b** and **B2c**.

residues while hydrogen bonding is weak and non-existent in the macrocycle residue of erythromycin **2** and erythralosamine **4**.

It is concluded that NMR spectroscopy is a powerful method for the determination of the solution conformations of macrolide antibiotics. However some minor conformations, **A2e**, **A1d** and **B1b** are present to only a small extent and it is therefore difficult to characterize them with certainty. Furthermore molecular dynamics and mechanics calculations are very useful for comparing these solution-state conformations derivatives and generating different models.

Consequently, this study highlights the influence of other factors that may explain some of the significant differences between these two antibiotics.

Experimental

NMR Spectroscopy.—The experiments were carried out at 250 and 500 MHz for ^1H and 62.9 MHz for ^{13}C, on Bruker WM 250 and AM 500 Spectrometers at 300 K using a sample concentration of 5×10^{-2} mol dm^{-3} in $CDCl_3$ solution. The samples were dissolved in deuterium oxide at a saturating concentration of *ca.* 0.01 mol dm^{-3} and [$^2H_4$] TSP was used as an internal reference for the proton shifts. Degassed and sealed tubes were used for the T_1 determinations and ^1H NOESY experiment. 2D ^1H–^{13}C COLOC spectra were acquired with sweep widths of 12 000 Hz into 4096 data points in f2; 128 evolution increments were used. A polarization delay time for long range coupling of 58 ms and a refocussing delay of 29 ms were implemented as was a relaxation delay of 1.5 s. Measurements of long-range heteronuclear (^{13}C–^1H) coupling constants were performed either on the WM250 spectrometer [15] using 2D selective INEPT on a sample of 60 mg in 0.75 cm^3 of $CDCl_3$ or at 500 MHz. At 500 MHz, selectivity was achieved by a 180° DANTE type pulse train *via* the decoupler channel with 40 short hard pulses of 5.4 μs and delays of 300 μs. Selectivity was equal to $\Delta\nu$ ^1H ± 50 Hz ($\gamma B_1/2\pi$ = 50 Hz). The 90° non-selective proton pulses were 63 μs. D3 was thus set to 50 ms corresponding to $1/nJ_{CH}$ with $J_{CH} \approx 3$ Hz. The relaxation delay was 1.3 s and each FID was acquired with 64 scans with broad-band decoupling. 64 experiments were carried out then data were zero-filled to 256 points in the F1 dimension. In the F2 dimension, data were acquired with 2048 points and no zero-filling was applied. Resolution enhancement by Gaussian transformation was realized in F2 and F1 dimensions. The D_0 delay was initially set to a value of 3×10^{-6} s and was increased by 17 ms between each experiment.

Molecular Dynamics.—The calculations were run on a Silicon Graphics computer using the Biosym software 'INSIGHT II' and 'DISCOVER'.

The structures were derived from the crystallographic coordinates of the solid **1** and **2** as a starting point and the substituents and the charges were modified. For the molecular dynamics calculations, the trajectories were calculated by means of the Verlet Algorithm used in the force-field of DISCOVER. The starting structures were first minimized using 100 steps of the 'Steepest Descent' algorithm and then the 'Conjugate Gradients' algorithm until a convergence of 0.1 kcal mol^{-1} was reached. The system was then equilibrated over a period of 4 ps to reach a temperature of 300 K by coupling it to a thermal bath.[32] The dynamics were run for 40 ps (variable temperature) or 100 ps (constant temperature), the trajectory was sampled by minimizing and storing the structure every pico-second.

For the electrostatic energies, since no explicit solvent molecules were incorporated during the run, the relative permittivity was set distance-dependant ($\varepsilon = R_{ij}$), in order to mimic the solvent effect.

When a molecular dynamics simulation was performed on the protonated compounds, charges and atomic potentials were then redefined for the protonated molecules using the built-in algorithm of the program.[33]

Products.—Erythromycin, roxithromycin and RU39001 were kindly provided by *Laboratoire Roussel Uclaf* (Paris); erythralosamine was synthesized according to E. H. Flynn *et al.*[24]

Acknowledgements

We thank *Laboratoire Roussel* (Paris) for their scientific and financial support during this research.

References

1 H. A. Kirst, *Ann. Rep. Med. Chem.*, 1989, **25**, 119.
2 T. Cachet, G. Van den Mooter, R. Hauchecorne, C. Vinckier and J. Hoogmartens, *Int. J. Pharm.*, 1989, **55**,59; 1989, **55**, 67.
3 (*a*) J. R. Everett and E. Hunt, *J. Chem. Soc., Perkin Trans. 2*, 1991,

1481; (*b*) D. A. Pye, J. I. Gyi and J. Barber, *J. Chem. Soc., Chem. Commun.*, 1990, 1143.
4 E. G. Brain, A. K. Forrest, E. Hunt, C. Shillingford and J. M. Wilson, *J. Antibiot.*, 1989, **42**, 1817.
5 J. F. Chantot, J. C. Gasc, S. Goin D'Ambrieres and A. Lutz, *23rd Interscience Conference on Antimicrobial Agents in Chemotherapy*, 1983, Abstr. 447, Las Vegas, USA.
6 J. F. Chantot, A. Bryskier and J. C. Gasc, *J. Antibiot.*, 1986, **39**, 660.
7 M. Delaforge, E. Sartori and D. Mansuy, *Chem.-Biol. Interact.*, 1988, **68**, 179.
8 (*a*) I. O. Kibwage, R. Busson, G. Janssen, J. Hoogmartens and H. Vanderhaeghe, *J. Org. Chem.*, 1987, **52**, 990; (*b*) K. Tsuji, *J. Chromatogr.*, 1978, **158**, 337.
9 E. Sartori, M. Delaforge and D. Mansuy, *Biochem. Pharm.*, 1989, **38**, 2061.
10 'Roxithromycin: a New Macrolide', Special issue of *J. Antimicrob. Chemother.*, 1987, **20**, Suppl. B.
11 F. Kees, H. Grobecker, J. B. Fourtillan, D. Tremblay and B. Saint Salvi, *Br. J. Clin. Pract.*, 1988, **55**, 51.
12 A. McLean, J. A. Sutton, J. Salmon and D. Chatelet, *Br. J. Clin. Pract.*, 1988, **55**, 52.
13 M. Delaforge and E. Sartori, *Biochem. Pharmacol.*, 1990, **40**, 223.
14 J. Gharbi-Benarous, M. Delaforge, I. Artaud and J. P. Girault, *Magn. Reson. Chem.* 1990, **28**, 846.
15 J. Gharbi-Benarous, P. Ladam, M. Delaforge and J. P. Girault, *J. Chem. Soc., Perkin Trans. 2*, 1992, 1989.
16 (*a*) M. Delaforge, P. Ladam, G. Bouillé, J. Gharbi-Benarous, M. Jaouen and J. P. Girault, *Chem.-Biol. Interact.*, 1992, 215; (*b*) J. Gharbi-Benarous, M. Delaforge, C. K. Jankowski and J. P. Girault, *J. Med. Chem.*, 1991, **34**, 1117.
17 B. Bachet, C. Brassy and J. P. Mornon, *Acta Crystallogr., Sect. C, Cryst. Struct. Commun.*, 1988, **44**, 112.
18 D. R. Harris, S. G. McGeachin and H. H. Mills, *Tetrahedron Lett.*, 1965, **11**, 679.
19 C. Manuel, P. Delamonica, M. J. Rosset, C. Safran, D. Pirot, L. Audegond, J. C. Pechere, '16th International Congress of Chemotherapy', 1989, Abstr. 1224, Jerusalem; B. J. Luft and J. S. Remington, *J. Infect. Dis.*, 1988, **157**, 1.
20 (*a*) J. R. Everett and J. W. Tyler, *J. Chem. Soc., Perkin Trans 2*, 1987, 1659; *J. Chem. Soc., Perkin Trans. 2*, 1988, 325; (*b*) J. R. Everett and J. W. Tyler, *J. Chem. Soc., Chem. Soc.*, 1987, 815; (*c*) J. R. Everett and J. W. Tyler, *Magn. Reson. Chem.*, 1988, *26*, 179.
21 A. Nakagawa and S. Omura, *Macrolide Antibiotics. Chemistry, Biology and Practice*, ed. S. Omura, Academic Press, Orlando, 1984, p. 75.
22 J. Mulzer, H. M. Kirstein, J. Buschmann, C. Lehmann and P. Luger, *J. Am. Chem. Soc.*, 1991, **113**, 910.
23 R. S. Egan, T. J. Perun, J. R. Martin and L. A. Mitscher, *Tetrahedron*, 1973, **29**, 2525; T. J. Perun, R. S. Egan and J. R. Martin, *Tetrahedron Lett.*, 1969, 4501.
24 V. Rutar, *J. Magn. Reson.*, 1984, **58**, 306; T. C. Wong and V. Rutar, *J. Am. Chem. Soc.*, 1984, **106**, 7380.
25 H. Kessler, C. Griesinger and J. Lautz, *Angew. Chem., Int. Ed. Engl.*, 1984, **23**, 444.
26 J. G. Nourse and J. D. Roberts, *J. Am. Chem. Soc.*, 1975, **97**, 4584.
27 P. Ladam, J. Gharbi-Benarous, M. Pioto, M. Delaforge and J. P. Girault, *Magn. Reson. Chem.*, 1992. submitted.
28 I. Tvaroska, M. Hricovini, E. Petrakova, *Carbohydr. Res.*, 1989, **189**, 359.
29 D. Marion and K. Wuthrich, *Biochem. Biophys. Res. Commun.*, 1983, **113**, 976.
30 A. Allerhand, D. Doddrell and R. Komoroski, *J. Chem. Phys.*, 1971, **55**, 189; J. R. Lyerla and G. C. Levy, *Top. Carbon-13 NMR Spectrosc.*, 1974, **1**, 79.
31 P. Dauber-Osguthorpe, V. A. Roberts, D. J. Osguthorpe, J. Wolff, M. Genest and A. T. Hagler *Proteins: Struct., Funct. Genet.*, 1988, **4**, 31.
32 H. J. C. Berendsen, J. P. M. Postma, W. F. van Gunsteren, A. DiNola and J. R. Haak, *J. Chem. Phys.*, 1984, **81**, 3684.
33 U. Dinur and A. T. Hagler, *J. Chem. Phys.*, 1989, **91**, 2949.
34 E. H. Flynn, M. V. Sigal and K. Gerson, *J. Am. Chem. Soc.*, 1954, **76**, 3121.

Paper 3/01654D
Received 22*nd March* 1993
Accepted 1*st July* 1993

CONFERENCE DIARY†

1993

November

Florida Environmental Chemistry Conference, Palm Coast, FL, USA **November 1–5**

Contact: Professor R. S. Drago, Department of Chemistry, University of Florida, Gainesville, FL 32611, USA
Fax +1 904 392 8758

Finnish Chemical Congress, Helsinki, Finland
November 2–4

Contact: Association of Finnish Chemical Societies, Hietaniemenkatu 2, SF-00100, Helsinki, Finland
Tel +358 (0) 408 022. Fax +358 (0) 408 780

Applied Organometallic Chemistry, München, Germany
November 4–5

Contact: COMST, POB 415, 1001 Lausanne 1, Switzerland
Tel +41 21 23 4886. Fax +41 21 234972

Environmentally Friendly Chemistry using Supported Reagent Catalysts, Scientific Societies Lecture Theatre, London, UK
November 23

RSC* (Mr. S. S. Langer)

December

Organometallics in Synthesis—An Element of Choice, Belgrave Sq., London, UK **December 1**

Contact: Dr. M. J. Rice, Zeneca Agrochemicals, Jealots Hill Research Station, Bracknell, Berkshire, UK RG12 6EY
Tel +44 (0) 344 414855. Fax +44 (0) 344 55629

3rd Tohwa University International Symposium on Synthetic and Mechanistic Hydrocarbon Chemistry, Fukuoka, Japan **December 6–9**

Contact: Professor Dr. Y. Nagano, Tohwa Institute of Science, Tohwa University, Fukuoka 815, Japan
Fax +81 92 542 0813

27th Annual Meeting on Modern Aspects of Stereochemistry, Sheffield, UK **December 15**

Contact: Professor C. J. M. Stirling, Department of Chemistry, The University of Sheffield, Sheffield, UK S3 7HF
Tel +44 (0) 742 768555. Fax +44 (0) 742 738673

Free Radicals, Antioxidants, Lipids and Health, Belgrave Sq., London, UK **December 15**

Contact: SCI, Conference Dept., 14/15 Belgrave Sq., London, UK SW1X 8PS
Tel +44 (0) 71 235 3681. Fax +44 (0) 71 823 1698

Potential Energy Surfaces and Organic Reaction Paths, Oxford, UK **December 15–17**

RSC* (Mrs. Y. A. Fish)

1994

January

Natural Products and Medicinal Chemistry, Kingston, Jamaica **January 3–7**

Contact: Organising Secretary, Mona Symposium, Department of Chemistry, University of the West Indies, Mona, Kingston 7, Jamaica

Dynamics, Kinetics and Rate Equations in Heterogeneous Catalysis, Manchester, UK **January 6–7**

RSC* (Mr. S. S. Langer)

---

* *Contact:* Dr. J. F. Gibson, Royal Society of Chemistry, Burlington House, Piccadilly, London, UK W1V 0BN. Fax +44 (0) 71 437 8883.
† Conference organisers are invited to provide details of meetings concerning organic, bio-organic or physical organic chemistry to: Dr. A. P. Kybett, Journals Department, Royal Society of Chemistry, Thomas Graham House, Science Park, Cambridge, UK CB4 4WF.

19th International Symposium on the Chemistry of Natural Products, Karachi, Pakistan **January 16–20**	*Contact:* Professor Atta-ur-Rahman, H.E.J. Research Institute of Chemistry, University of Karachi, Karachi-75270, Pakistan Tel +92 21 470007. Fax +92 21 467887 E-mail atta%hejfirst@unet.uu.net
Trombay Symposium on Radiation and Photochemistry, Bombay, India **January 17–21**	*Contact:* Dr. S. N. Guha, Secretary, Symposium Organising Committee Chemistry Division, BARC, Bombay 400 085, India Tel +91 22 556 3060 ext. 2280. Fax +91 22 556 0750
Renewable Resource Building Blocks for Polymer Science, SCI, London, UK **January 26**	RSC* (Mrs. Y. A. Fish)

March

Biotransformations in Action: A Practically Based Course on Opportunities and Techniques in Biocatalysis for Synthetic Organic Chemists, Blacksburg, VA, USA **March 3–7**	*Contacts:* Professor T. Hudlicky, Department of Chemistry, Virginia Polytechnic & State University, Blacksburg, VA 24061, USA *or* Professor S. M. Roberts, Department of Chemistry, University of Exeter, Stocker Road, Exeter, UK EX4 4QD
Reductions in Organic Synthesis, Scientific Societies Lecture Theatre, London, UK **March 15**	*Contact:* Dr. K. T. Veal, SmithKline Beecham, Coldharbour Road, Harlow, Essex, UK CM19 5AD Tel +44 (0) 279 622269. Fax +44 (0) 279 622348
Physical Methods in Bioorganic Chemistry, Scientific Societies Lecture Theatre, London, UK **March 21**	RSC*
ESR Conference, Cardiff, UK **March 21–25**	*Contact:* Dr. C. C. Rowlands, School of Pure and Applied Chemistry, University of Wales College of Cardiff, PO Box 912, Cardiff, UK CF1 3TB Tel +44 (0) 222 874073. Fax +44 (0) 222 874030
Fatty Acid Biosynthesis, Belgrave Square, London, UK **March 22**	*Contact:* Dr. D. W. Holloman Tel +44 (0) 275 392 181. Fax +44 (0) 275 394 007

April

RSC Annual Congress (Horizons for Organic Chemistry in the 21st Century), Liverpool, UK **April 12–15**	RSC*
Transition Metals in Supramolecular Chemistry, Genoa, Italy **April 14–16**	*Contact:* Professor Luigi Fabrizzi, NATO ARW, Dipartimento di Chimica Generale, Viale Taramelli, 12, I-27100 Pavia, Italy Tel +39 382 392328. Fax +39 382 528544
Converging Methods for Determining Polypeptide Structures, Gregynog, UK **April 15–17**	RSC*
Florida Catalysis Conference, Palm Coast, FL, USA **April 18–22**	*Contact:* Professor R. S. Drago, Department of Chemistry, University of Florida, Gainesville, FL 32611, USA Fax +1 904 392 8758
5th Medicinal Chemistry Symposium, Hatfield, UK **April 21**	Dr. D. I. C. Scopes, Medicinal Chemistry Department, Glaxo Group Research Ltd., Park Road, Ware, Herts, UK SG12 0DP Tel +44 (0) 920 882656
Synthesis of Medicinally Important Carbohydrates and Analogues, Exeter, UK **April 21–22**	RSC*

---

* *Contact:* Dr. J. F. Gibson, Royal Society of Chemistry, Burlington House, Piccadilly, London, UK W1V 0BN. Fax +44 (0) 71 437 8883

May

29th ESF/Euchem Conference on Stereochemistry, Bürgenstock, Switzerland **May 1–7**	*Contact:* Professor A. Pfaltz, Institute of Inorganic Chemistry, University of Basel, St Johannsring 19, CH 4056, Basel, Switzerland

June

12th European Experimental NMR Conference, Oulu, Finland **June 5–10**	*Contact:* Dr. Petri Ingman, Department of Chemistry, University of Oulu, FIN-90570, Oulu, Finland Tel +358 81 553 1622. Fax +358 81 553 1603
25th Reaction Mechanisms Conference, Notre Dame, IN, USA **June 10–15**	*Contact:* Dr. Daniel J. Pasto, 1994 Reaction Mechanisms Conference, Department of Chemistry and Biochemistry, University of Notre Dame, Notre Dame, IN 46556, USA Fax +1 219 631 6652
XIX International Symposium on Macrocyclic Chemistry, Lawrence, KS, USA **June 13–17**	*Contact:* Professor Daryle H. Busch *or* Kristen Bowman-James, Department of Chemistry, University of Kansas, Lawrence, KS 66045, USA

July

2nd International Symposium on Supported Reagents and Catalysts in Chemistry, Swansea, UK **July 5–8**	RSC*
16th International Conference on Organometallic Chemistry, Brighton, UK **July 10–15**	RSC*
35th IUPAC International Symposium on Macromolecules, Akron, OH, USA **July 11–15**	*Contact:* Cathy Manus-Gray, MacroAkron '94, The University of Akron, Akron, OH 44325-3909, USA Tel +1 216 972 5334. Fax +1 216 972 5463 E-mail Manusgray@uakron.edu
5th Belgian Organic Synthesis Symposium, Namur, Belgium **July 11–15**	*Contact:* Professor A. Krief, Facultés Universitaires Notre Dame de la Paix, Department of Chemistry, 61, rue de Bruxelles, B-5000 Namur, Belgium Tel +32 81 72 45 39. Fax +32 81 72 45 36
17th International Carbohydrate Symposium, Ottawa, Canada **July 17–22**	*Contact:* Dr. H. Jennings, Institute of Biological Sciences, National Research Council of Canada, 100 Sussex Drive, Ottawa, Ontario, Canada K1A OR6
Recognition Processes, Birmingham, UK **July 24–29**	RSC*
8th International Symposium on Molecular Recognition and Inclusion, Ottawa, Canada **July 31–August 5**	*Contact:* Mrs. Huguette Morin-Dumais, Steacie Institute for Molecular Sciences, National Research Council of Canada, 100 Sussex Drive, Ottawa, Ontario, Canada, K1A 0R6 Tel +1 613 990 0936. Fax +1 613 954 5242 E-mail ISMRI@NED1.SIMS.NRC.CA

August

Physical Organic Principles Applied to Supramolecular Chemistry. From Bioorganic Structures to New Materials, Geneva, Switzerland **August 25–28**	*Contact:* Professor P. Müller, Département de Chimie Organique, Université de Genève, 30, quai Ernest-Ansermet, CH-1211 Genève 4 Tel +41 (0) 22 702 6527. Fax +41 (0) 22 328 7396 E-mail MULLER@SC2A.UNIGE.CH

* *Contact:* Dr. J. F. Gibson, Royal Society of Chemistry, Burlington House, Piccadilly, London, UK W1V 0BN. Fax +44 (0) 71 437 8883

12th International Conference on Physical Organic Chemistry, Padova, Italy **August 28–September 2**

Contact: Professor G. Scorrano, Dipartimento Di Chimica Organica, Universita degli Studi di Padova, Via Marzolo 1, 35100 Padova, Italy. Fax +39 49 831222

September

RSC Autumn Meeting [Organic Chemistry: Synthesis and Mechanisms (i) Mechanisms in Molecular Recognition and Bioorganic Chemistry (ii) Physical Organic Chemistry and Synthetic Methodology (iii) Organometallics in Organic Synthesis], Glasgow, UK **September 6–9**

RSC*

International Symposium on Cascade Reactions, Leeds, UK **September 12–14**

RSC*

6th Symposium on the Latest Trends in Organic Synthesis, Blacksburg, VA, USA **September 28–October 2**

Contact: Professor Tomas Hudlicky, Department of Chemistry, Virginia Polytechnic Institute and State University, Blacksburg, VA 24061-0212, USA
Tel +1 703 231 4509. Fax +1 703 231 3941

October

First Swiss Course on Medicinal Chemistry, Leysin, Switzerland **October 9–14**

Contact: Dr. Han van de Waterbeemd, F. Hoffmann-La Roche Ltd., CH-4002 Basel, Switzerland
Tel +41 61 688 8421. Fax +41 61 688 1745

November

Biotransformations in Action: A Practically Based Course on Opportunities and Techniques in Biocatalysis for Synthetic Organic Chemists, Blacksburg, VA, USA **November 3–7**

Contacts: Professor T. Hudlicky, Department of Chemistry, Virginia Polytechnic & State University Blacksburg, VA 24061, USA *or* Professor S. M. Roberts, Department of Chemistry, University of Exeter, Stocker Road, Exeter, UK EX4 4QD

6th International Kyoto Conference on New Aspects of Organic Chemistry, Kyoto, Japan **November 7–11**

Contact: Professor Yoshihiko Ito, Chairman IKCOC-6, Department of Synthetic Chemistry, Kyoto University, Yoshida, Kyoto 606-01, Japan

December

10th International Conference on Organic Synthesis, Bangalore, India **December 11–16**

Contact: Professor G. S. R. Subba Rao, Department of Organic Chemistry, Indian Institute of Science, Bangalore 560 012, India
Tel +91 80 344411. Fax +91 80 341683
E-mail Ocgsrs@orgchem.iisc.ernet.in

28th Annual Meeting on Modern Aspects of Stereochemistry, Sheffield, UK **December 14**

Contact: Professor C. J. M. Stirling, Department of Chemistry, The University of Sheffield, Sheffield, UK S3 7HF
Tel +44 (0) 742 768555. Fax +44 (0) 742 768555

1995

March

Lipophilicity in Drug Research and Toxicology, Lausanne, Switzerland **March 21–24**

Contact: Professor Bernard Testa, School of Pharmacy, University of Lausanne, BEP, CH-1015 Lausanne, Switzerland
Tel +41 21 692 2851. Fax +41 21 692 2880

April

RSC Annual Congress, Edinburgh, UK **April 10–13**

RSC*

---

* *Contact:* Dr. J. F. Gibson, Royal Society of Chemistry, Burlington House, Piccadilly, London, UK W1V 0BN. Fax +44 (0) 71 437 8883

International Symposium on Protein Structure and Function, Exeter, UK **April 19–21**	*Contact:* Professor S. M. Roberts, Department of Chemistry, University of Exeter, Stocker Road, Exeter, UK EX4 4QD Tel +44 (0) 392 263429/30. Fax +44 (0) 392 263431

July

12th International Meeting: NMR Spectroscopy, Manchester, UK **July 2–7**	RSC*
XXth International Symposium on Macrocyclic Chemistry, Jerusalem, Israel **July 2–7**	*Contact:* Secretariat, XXth International Symposium on Macrocyclic Chemistry, PO Box 50006, Tel Aviv 61500, Israel Tel +972 3 5140014. Fax +972 5175674
Biological Challenges for Organic Chemistry, St Andrews, UK **July 10–13**	RSC*
International Society of Magnetic Resonance Conference, Sydney, Australia **July 16–21**	*Contact:* Dr. Les Field, Chairman, ISMAR-95, Department of Organic Chemistry, University of Sydney, Sydney, NSW 2006, Australia. Tel +61 2 692 2060. Fax +61 2 692 3329 E-mail ISMAR-95@biochem.su.oz.au
14th International Symposium—Synthesis in Organic Chemistry, Cambridge, UK **July 24–27**	RSC*

August

IUPAC General Assembly, Guildford, UK **August 7–15**	RSC*

September

8th Medicinal Chemistry Symposium, Cambridge, UK **September 10–13**	RSC* (Mr. S. S. Langer)

December

Pacifichem '95 (International Congress of Pacific Basin Chemical Societies), Honolulu, HI, USA **December 17–22**	*Contact:* Mrs. C. Pruitt, Congress Manager Pacifichem '95, American Chemical Society, 1155–16th St., NW, Washington DC 20036, USA Tel +1 202 872 4397. Fax +1 202 872 6128 E-mail cpp91@acs.org

* *Contact:* Dr. J. F. Gibson, Royal Society of Chemistry, Burlington House, Piccadilly, London, UK W1V 0BN. Fax +44 (0) 71 437 8883

DIARY OF MAJOR MEETINGS OF THE AMERICAN CHEMICAL SOCIETY

MEETING	YEAR	DATE	LOCATION
207th	Spring 1994	March 13–18	San Diego, CA
208th	Fall 1994	August 21–26	Washington, DC
209th	Spring 1995	April 2–7	Anaheim, CA
210th	Fall 1995	August 20–25	Chicago, IL
211th	Spring 1996	March 24–29	Seattle, WA
212th	Fall 1996	August 25–30	Boston, MA
213th	Spring 1997	April 6–11	San Antonio, TX
214th	Fall 1997	September 7–12	Las Vegas, NV
215th	Spring 1998	March 29–April 3	St. Louis, MO
216th	Fall 1998	August 23–28	Orlando, FL
217th	Spring 1999	March 21–26	Anaheim, CA
218th	Fall 1999	August 22–27	New Orleans, LA
219th	Spring 2000	March 26–31	Las Vegas, NV
220th	Fall 2000	August 20–25	Washington, DC
221st	Spring 2001	April 1–6	San Francisco, CA
222nd	Fall 2001	August 19–24	Chicago, IL

Contact: ACS Meetings, 1155–16th St., N.W. Washington DC 20036–4899, USA

---

* *Contact:* Dr. J. F. Gibson, Royal Society of Chemistry, Burlington House, Piccadilly, London, UK W1V 0BN. Fax +44 (0) 71 437 8883